Molecular Plant
Research article

CellPress
Partner Journal

Arsenite provides a selective signal that coordinates arsenate uptake and detoxification through the regulation of PHR1 stability in *Arabidopsis*

Cristina Navarro[1,7], Cristian Mateo-Elizalde[1,7], Thotegowdanapalya C. Mohan[1,4,7], Eduardo Sánchez-Bermejo[1,5], Oscar Urrutia[2], María Nieves Fernández-Muñiz[3], José M. García-Mina[2], Riansares Muñoz[3], Javier Paz-Ares[1], Gabriel Castrillo[1,6,*] and Antonio Leyva[1,*]

[1]Department of Plant Molecular Genetics, Centro Nacional de Biotecnología-Consejo Superior de Investigaciones Científicas, Madrid 28049, Spain

[2]Department of Environmental Biology, Sciences School, University of Navarra, Pamplona 31008, Spain

[3]Department of Analytical Chemistry, School of Chemical Sciences, Universidad Complutense de Madrid, Madrid 28040, Spain

[4]Present address: Department of Biotechnology and Bioinformatics, Faculty of Life Sciences, JSS Academy of Higher Education and Research, Mysuru, Karnataka 570015, India

[5]Present address: S&A Fresh Produce. Brook Farm, Marden, Hereford HR1 3ET, UK

[6]Present address: Future Food Beacon of Excellence & School of Biosciences, University of Nottingham, Nottingham LE12 5RD, UK

[7]These authors contributed equally to this article.

***Correspondence: Gabriel Castrillo (gabriel.castrillo@nottingham.ac.uk), Antonio Leyva (aleyva@cnb.csic.es)**

https://doi.org/10.1016/j.molp.2021.05.020

ABSTRACT

In nature, plants acquire nutrients from soils to sustain growth, and at the same time, they need to avoid the uptake of toxic compounds and/or possess tolerance systems to cope with them. This is particularly challenging when the toxic compound and the nutrient are chemically similar, as in the case of phosphate and arsenate. In this study, we demonstrated that regulatory elements of the phosphate starvation response (PSR) coordinate the arsenate detoxification machinery in the cell. We showed that arsenate repression of the phosphate transporter *PHT1;1* is associated with the degradation of the PSR master regulator PHR1. Once arsenic is sequestered into the vacuole, PHR1 stability is restored and *PHT1;1* expression is recovered. Furthermore, we identified an arsenite responsive SKP1-like protein and a PHR1 interactor F-box (PHIF1) as constituents of the SCF complex responsible for PHR1 degradation.We found that arsenite, the form to which arsenate is reduced for compartmentalization in vacuoles, represses *PHT1;1* expression, providing a highly selective signal versus phosphate to control *PHT1;1* expression in response to arsenate. Collectively, our results provide molecular insights into a sensing mechanism that regulates arsenate/phosphate uptake depending on the plant's detoxification capacity.

Key words: arsenic signaling, F-box protein, arsenate uptake, arsenic detoxification, phosphate starvation, phytoremediation

Navarro C., Mateo-Elizalde C., Mohan T.C., Sánchez-Bermejo E., Urrutia O., Fernández-Muñiz M.N., García-Mina J.M., Muñoz R., Paz-Ares J., Castrillo G., and Leyva A. (2021). Arsenite provides a selective signal that coordinates arsenate uptake and detoxification through the regulation of PHR1 stability in *Arabidopsis*. Mol. Plant. **14**, 1–19.

INTRODUCTION

Plant roots must face continuous changes in the soil environment that require fast and tight control of transporters to modulate the uptake of nutrients and toxic compounds present in soil patches. In particular, several metal and metalloid transporters are able to incorporate both essential and nonessential toxic metals and metalloids, together with macronutrients (Korshunova et al.,

Published by the Molecular Plant Shanghai Editorial Office in association with Cell Press, an imprint of Elsevier Inc., on behalf of CSPB and CEMPS, CAS.

Please cite this article in press as: Navarro et al., Arsenite provides a selective signal that coordinates arsenate uptake and detoxification through the regulation of PHR1 stability in *Arabidopsis*, Molecular Plant (2021), https://doi.org/10.1016/j.molp.2021.05.020

1999; Thomine et al., 2000; Shin et al., 2004; Sors et al., 2005; Ma et al., 2008; Zhao et al., 2010c; Himeno et al., 2019). Therefore, in plants, the coincidence of both toxic and nontoxic compounds in soils requires the existence of precise systems that distinguish between beneficial nutrients and toxic elements with high chemical similarities. Despite the critical importance of these rescue systems for plant survival and distribution, their underlying molecular mechanisms are mostly unknown.

Today, arsenic is one of the most important carcinogens present in soils and groundwater that threaten all organisms (International Agency for Research on Cancer, IARC, 2012). In plants, arsenate [As(V)] and arsenite [As(III)], the most abundant chemical forms of arsenic present in the biosphere, are easily incorporated into cells (Catarecha et al., 2007; Ma et al., 2008; Kamiya et al., 2009; Wu et al., 2011; LeBlanc et al., 2013; Xu et al., 2015), facilitating the entry of the metalloid into the food chain and thus threatening the health of millions of people (Meharg and Rahman, 2003; Williams et al., 2006; Zhu et al., 2008; Zhao et al., 2010b and references therein). As(V) toxicity is due primarily to its close chemical similarity to phosphate (Pi), and therefore its pernicious effects come from its ability to interfere with Pi metabolism (Long and Ray, 1973; Gresser, 1981). Because of this structural analogy, As(V) is easily incorporated into cells through the plant's high-affinity Pi transport system (Meharg and Macnair, 1992a; Meharg and Hartley-Whitaker, 2002; Shin et al., 2004). Once inside the cell, As(V) is rapidly reduced to highly toxic As(III) through the action of arsenate reductases, particularly ARQ1/HAC1 (Chao et al., 2014; Sánchez-Bermejo et al., 2014). Nevertheless, As(III) is quickly sequestered into the vacuoles complexed with phytochelatins (Grill et al., 1987; Sneller et al., 1999; Schmöger et al., 2000; Tripathi et al., 2007; Indriolo et al., 2010; Liu et al., 2010; Song et al., 2010) or extruded through Nod26-like aquaporins or auxin transporters (Bienert et al., 2008; Verbruggen et al., 2009; Zhao et al., 2010a; Ashraf et al., 2020).

In soils, the amount of Pi available is often extremely low, below 10 μM (Holford, 1997). It is well known that at this concentration, plants enter a Pi-starvation state that activates the phosphate starvation response 1 (PHR1) transcription factor, which controls the expression of the *PHT1* high-affinity Pi/As(V) transporters (Rubio et al., 2001; Bustos et al., 2010). This response provokes an immediate localization of the transporters to the plasma membrane (Chen et al., 2015), leaving plants ready to capture Pi. Therefore, we must consider that in most soils, plants may constitutively express the Pi/As(V) transporters. In arsenic-contaminated soils, plants are therefore highly susceptible to As(V) toxicity and must be able to sense both anions. This is particularly relevant to the coordination of Pi/As(V) uptake with As(V) detoxification in order to achieve efficient plant tolerance to high As(V) and low Pi soils. In nature, plants have developed an extraordinary ability to restrict As(V) uptake once the metalloid is perceived (Meharg and Macnair, 1992b; Castrillo et al., 2013). Restriction of *PHT1* expression in response to As(V) might lead to a conflict wherein the benefits of As(V) uptake restriction compromise the acquisition of Pi, an essential nutrient for plant growth and reproduction. In the model plant *Arabidopsis thaliana* (*Arabidopsis*), decreased As(V) uptake involves the transcriptional repression of Pi transporters through the action of the transcription factor WRKY6 (Castrillo et al., 2013). Whether or not additional regulators function in the control of As(V) uptake in response to the metalloid is currently unknown.

In this study, we show that PHR1, the key regulator of the As(V)/Pi transporter *PHT1;1*, is rapidly degraded in response to As(V). Once As(V) is sequestered into the vacuole, PHR1 accumulation is quickly restored, which leads to the reactivation of *PHT1;1* expression. We identified an arsenic-induced SKP1-like protein (ASK18) and an F-box protein (PHIF1) as the SCF components that determine PHR1 stability and restoration. We also show that, similar to As(V), As(III) can also prompt PHR1 degradation and the induction of *WRKY6* and *ASK18* expression. We provide evidence supporting the notion that As(III) acts as an intracellular signal to promote arsenic responses, providing a checkpoint to adapt Pi/As(V) uptake to the arsenic detoxification capacity.

RESULTS

The amount of arsenate determines the time course of repression of *PHT1;1* expression

To further characterize the mechanisms underlying the repression of the Pi transporter *PHT1;1* in response to As(V), we analyzed its expression in wild-type *Arabidopsis* (accession Columbia-0, Col-0) plants treated with As(V) for 24 h. In line with our previous findings (Castrillo et al., 2013), *PHT1;1* was quickly repressed by 30 μM As(V) (Figure 1A). However, we observed that *PHT1;1* expression was restored after 24 h of As(V) treatment to levels similar to those of untreated plants. Similarly, the Pi transporter *PHO1,* involved in Pi xylem loading (Hamburger et al., 2002), was also repressed in response to As(V), and its expression was reactivated with expression kinetics identical to those of *PHT1;1* (Supplemental Figure 1). These observations suggest that Pi uptake recovery and distribution after As(V) exposure is tightly coordinated. As(V) dose-response experiments revealed that recovery of *PHT1;1* transcription is dependent on the initial As(V) concentration (Figure 1A). When the As(V) concentration was increased to 100 μM, the repression of *PHT1;1* expression was maintained after 24 h of As(V) exposure, which may indicate that *PHT1;1* recovery is dependent on the plant's capacity to detoxify As(V). In line with this notion, whole-plant arsenic quantification showed that after 24 h of As(V) exposure, arsenic was present mostly in plant tissues, reaching more than 530 μg/g DW, and barely detected in the medium (0.1 μg/mL) (Figure 1B). Therefore, despite being formally considered a non-hyperaccumulator plant, *Arabidopsis* showed an extraordinary ability to accumulate arsenic, and subsequently, as soon as the metalloid began to be removed from the medium and sequestered in vacuoles, *PHT1;1* transcription was rapidly restored (Figure 1A). Our results therefore revealed that *PHT1;1* expression recovery is associated with reduced As(V) levels in the external medium.

We have previously identified WRKY6 as the main repressor of *PHT1;1* expression in response to As(V) (Castrillo et al., 2013). Accordingly, *WRKY6* expression analysis performed in wild-type plants exposed to 30 μM As(V) (Figure 1C) showed that its expression kinetics are opposite to those observed for *PHT1;1* (Figure 1A). These results suggest that coordination of *PHT1;1*

Please cite this article in press as: Navarro et al., Arsenite provides a selective signal that coordinates arsenate uptake and detoxification through the regulation of PHR1 stability in *Arabidopsis*, Molecular Plant (2021), https://doi.org/10.1016/j.molp.2021.05.020

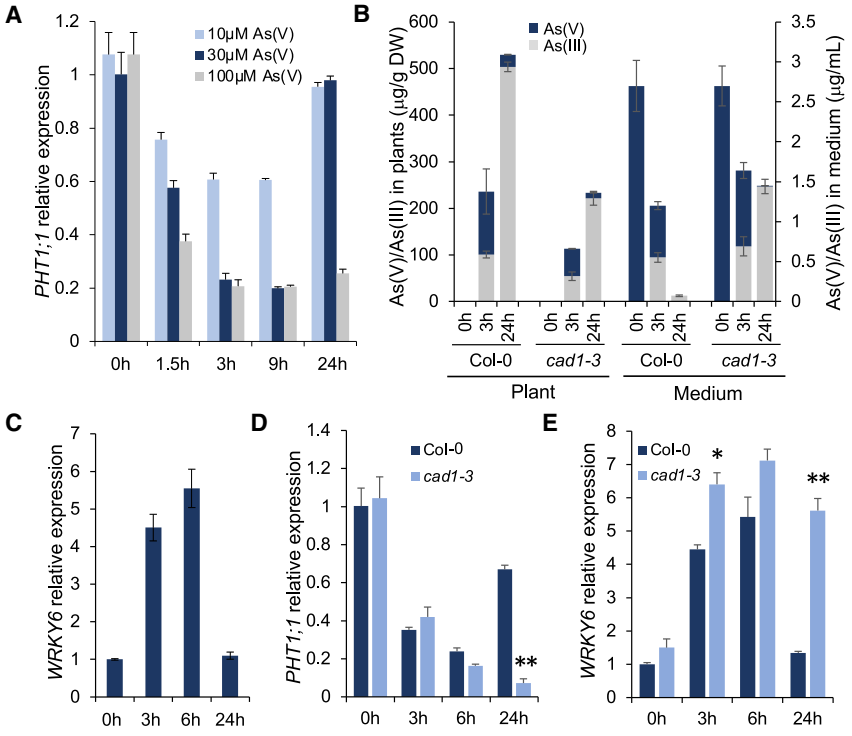

Figure 1. Arsenic detoxification capacity regulates *PHT1;1* expression.

(A) qRT-PCR analysis of the kinetic expression of *PHT1;1,* a Pi/As(V) transporter, in wild-type plants exposed to 10, 30, and 100 μM As(V). Wild-type plants were germinated on solid Johnson medium supplemented with 1 mM Pi for 7 days and then transferred to Pi-free medium for 2 additional days to induce the phosphate starvation response before the As(V) treatments. *PHT1;1* expression was analyzed in whole plants at 0, 1.5, 3, 9, and 24 h after the As(V) treatments.

(B) Quantification of arsenic chemical species, As(V) and As(III), in wild-type and *cad1-3* mutant plants. Plants were germinated and transferred as in (A) and then treated with 30 μM As(V). The arsenic analysis in the whole plant and in the medium was performed 0, 3, and 24 h after treatment with As(V). The data were normalized by the sample dry weight for plant tissue and by volume for the medium.

(C) qRT-PCR analysis of the kinetic expression of *WRKY6* in wild-type plants exposed to 30 μM As(V). Plants were germinated and transferred as in (A) and then treated with 30 μM As(V). Whole plants were collected at 0, 3, 6, and 24 h for analysis.

(D and E) qRT-PCR time course analysis of *PHT1;1* (D) and *WRKY6* (E) expression in wild-type (Col-0) plants and the *cad1-3* mutant. Plants were germinated and transferred as in (A) and then treated with 30 μM As(V). The expression of the genes was analyzed in whole plants collected at 0, 3, 6, and 24 h after treatment with As(V). Error bars indicate SD. *$p < 0.05$, **$p < 0.01$ (Student's t test versus the wild type). For all qRT-PCR experiments, we used three biological replicates, each consisting of 15 plants. For arsenic chemical species quantification, we used two independent biological replicates, each consisting of 45 plants.

expression with the amount of As(V) in the medium is determined by As(V)-mediated control of *WRKY6* expression. In order to substantiate the hypothesis that *PHT1;1* expression, and consequently As(V) uptake, adapts to the efficiency of the detoxification machinery, we performed qRT-PCR expression analysis on both genes in the *cad1-3* background. This mutant is altered in phytochelatin biosynthesis and is thus inefficient in sequestering As(III) into the vacuole. We therefore expected that *PHT1;1* expression recovery would be impaired in the *cad1-3* background. To demonstrate this, we began by quantifying the arsenic chemical species, As(V) and As(III), in mutant plants and media after 3 h and 24 h of As(V) exposure (Figure 1B). This experiment, performed in parallel with wild-type plants, showed that after 24 h of As(V) exposure, *cad1-3* accumulated less than half the As(III) accumulated in wild-type plants, and most was extruded back to the medium (Figure 1B). Under these conditions, *PHT1;1* expression was not restored after 24 h of As(V) treatment in the *cad1-3* mutant background, (Figure 1D), and accordingly, *WRKY6* transcript levels were maintained (Figure 1E). These results strongly suggest that the time course of repression of As(V)/Pi transporter *PHT1;1* expression is tightly coordinated with the plant's detoxification efficiency.

As(III) can act as a signal to modulate As(V) uptake

Quantification of arsenic chemical species in wild-type and *cad1-3* plants performed here (Figure 1B) and in previous studies (Liu et al., 2010; Chao et al., 2014; Sánchez Bermejo et al., 2014) showed that once As(V) enters the cell, it is rapidly transformed into As(III) by the action of arsenate reductases. This observation suggests that this chemical species may modulate *WRKY6* expression. Moreover, we observed that *WRKY6* transcript accumulation in response to As(V) treatment was higher in the *cad1-3* background than in wild-type plants. The high expression of *WRKY6* in *cad1-3* correlates with its increased As(III) accumulation (Figure 1B and 1E), suggesting that this chemical species regulates *WRKY6* expression.

We therefore decided to quantify *WRKY6* and *PHT1;1* expression in plants exposed to 60 μM As(III). qRT-PCR expression analysis showed that *WRKY6* responds to As(III) with kinetics similar to those found previously in response to As(V) (Figures 1C and 2A). Furthermore, *PHT1;1* also showed similar expression patterns in response to As(III) and As(V), not only in terms of repression but also in terms of reactivation (Figures 1A and 2B). To rule out the possibility that this effect is a consequence of the presence of As(V) in the medium owing to spontaneous As(III) oxidation (Park et al., 2016), we quantified the concentration of As(V) in the medium and also in the plant before and during our experiment (Supplemental Figure 2A). In all cases, the concentration of As(V) was below 550 nM, suggesting that spontaneous As(III) oxidation was negligible. qRT-PCR studies showed that plants exposed to 550 nM As(V) did not induce the expression of classical As(V)-regulated genes (Supplemental Figure 2B, 2C, and 2D) identified in our previous array (Castrillo et al., 2013). This result suggested that the oxidation of As(III) was minimal in the timeframe used for our experiments and that our transcript expression studies (Figure 2A and 2B) therefore reflect the plant response to As(III) and not to As(V). These observations indicate that As(III) can act as a signal of the arsenic response that modulates As(V) uptake through the action of WRKY6 on *PHT1;1* expression.

Please cite this article in press as: Navarro et al., Arsenite provides a selective signal that coordinates arsenate uptake and detoxification through the regulation of PHR1 stability in *Arabidopsis*, Molecular Plant (2021), https://doi.org/10.1016/j.molp.2021.05.020

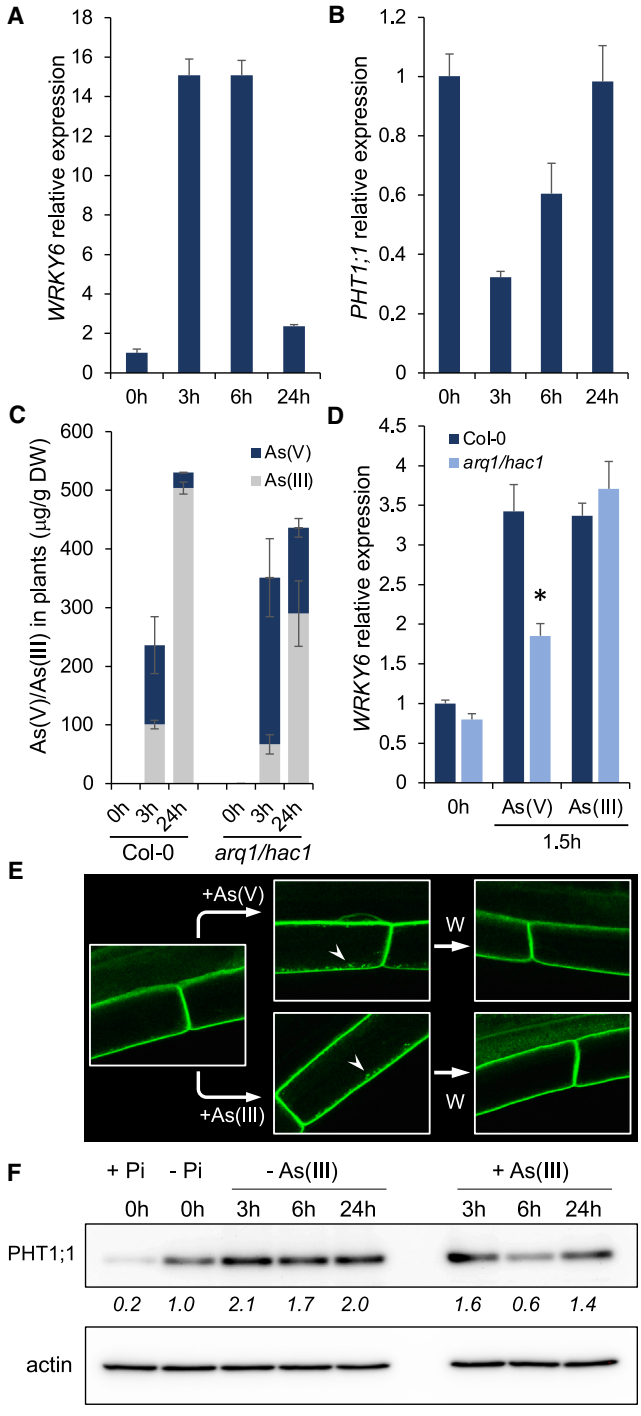

Figure 2. As(III) regulates expression and membrane localization of PHT1;1

(A and B) qRT-PCR analysis of the kinetic expression of *WRKY6* (A) and *PHT1;1* (B) in wild-type plants exposed to 60 µM As(III). Wild-type plants were germinated on solid Johnson medium supplemented with 1 mM Pi for 7 days and then transferred to Pi-free medium for 2 additional days to induce the PSR before As(III) treatment. Gene expression was analyzed in whole plants collected 0, 3, 6, and 24 h after treatment with 60 µM As(III).

(C) Quantification of arsenic chemical species, As(V) and As(III), in wild-type plants and the *arq1/hac1* mutant. Plants were germinated and transferred as in (A) and then treated with 30 µM As(V). The arsenic analysis was performed 0, 3, and 24 h after treatment with As(V) using the whole plant. The data were normalized by the sample dry weight.

We then hypothesized that *WRKY6* is tightly regulated by As(III) and that its downregulation therefore occurs only when the detoxification machinery efficiently copes with the As(III) present in the cytoplasm by sequestration of this toxic compound in the vacuole.

To obtain further evidence for the role of As(III) as a signal that controls As(V) uptake, we quantified arsenic chemical species in arsenate reductase *arq1/hac1* mutant plants exposed to 30 µM As(V) for 3 h and 24 h. This mutant is impaired in the reduction of As(V) to As(III) (Sánchez-Bermejo et al., 2014). We confirmed this impairment in Figure 2C: the conversion of As(V) to As(III) was 33% lower in the mutant background than in wild-type plants at 3 h and 42% lower at 24 h. Therefore, these mutant plants contain more As(V) and less As(III) than wild-type plants (Figure 2C). Hence, we expected that in *arq1/hac1*-mutant plants exposed to As(V), *WRKY6* transcriptional response would be reduced or increased, depending on whether the signal was As(III) or As(V), respectively. We therefore performed short-term qRT-PCR expression analysis of *WRKY6* in *arq1/hac1* mutants and wild-type plants exposed to As(V) and As(III). Whereas As(III) elicited a similar *WRKY6* expression response in wild-type and *arq1/hac1* mutant plants, the induction of *WRKY6* by As(V) was significantly reduced in *arq1/hac1* (Figure 2D), indicating that *WRKY6* is indeed regulated by As(III).

We also asked whether the localization of the PHT1;1 transporter is controlled by As(III), as has previously been shown for As(V) (Castrillo et al., 2013). We exposed *PHT1;1:GFP*-expressing plants to As(III) and determined PHT1; 1 subcellular localization using confocal microscopy (Figure 2E). We observed that similar to As(V), As(III) treatment led to PHT1;1 delocalization from the plasma membrane (Figure 2E). Furthermore, when plants were washed to remove As(V) and As(III) from the medium, PHT1;1 relocated at the plasma membrane. In parallel, we analyzed PHT1;1 protein accumulation in response

(D) qRT-PCR expression analysis of *WRKY6* in the *arq1/hac1* mutant background treated with 20 µM As(V) and 30 µM As(III). Plants were germinated and transferred as in (A) and then treated with 20 µM As(V) and 30 µM As(III). *WRKY6* expression was analyzed in whole plants collected 0 and 1.5 h after treatments. *$p < 0.05$ (Student's t test versus the wild type).

(E) Confocal analysis of PHT1;1:GFP localization in *A. thaliana* root epidermal cells. The analysis was performed using 5-day-old Pi-starved plants expressing *35S::PHT1;1:GFP*. For the confocal analysis, plants were treated with 30 µM As(V) ([+As(V)] or 60 µM As(III) [+As(III)], in liquid Johnson Pi-free medium (J-Pi) for 3 h. Plants were then washed (W) with water to remove As(V) or As(III) for 2 h. In the figure, arrowheads point to PHT1; 1-GFP internalization in vesicles.

(F) Immunoblot analyses of PHT1;1 protein levels in roots of plants expressing *35S::PHT1;1:GFP*. Plants were germinated on Johnson medium supplemented with 1 mM Pi for 7 days and then transferred to the same condition (+Pi) or to medium without Pi (−Pi) for 2 days. Plants from −Pi were subsequently treated with [+As(III)] or without [-As(III)] 90 µM As(III). For the analysis, roots were collected at 0, 3, 6, and 24 h after treatments. We used actin hybridization as a loading control. The numbers in italics below the lanes represent the adjusted relative intensity of the bands expressed relative to the −Pi condition and normalized to the corresponding loading control. In the figure, error bars indicate SD. For all qRT-PCR experiments, we used three independent biological replicates, each consisting of 15 plants. For arsenic chemical species quantification, we used two independent biological replicates, each consisting of 45 plants.

Please cite this article in press as: Navarro et al., Arsenite provides a selective signal that coordinates arsenate uptake and detoxification through the regulation of PHR1 stability in *Arabidopsis*, Molecular Plant (2021), https://doi.org/10.1016/j.molp.2021.05.020

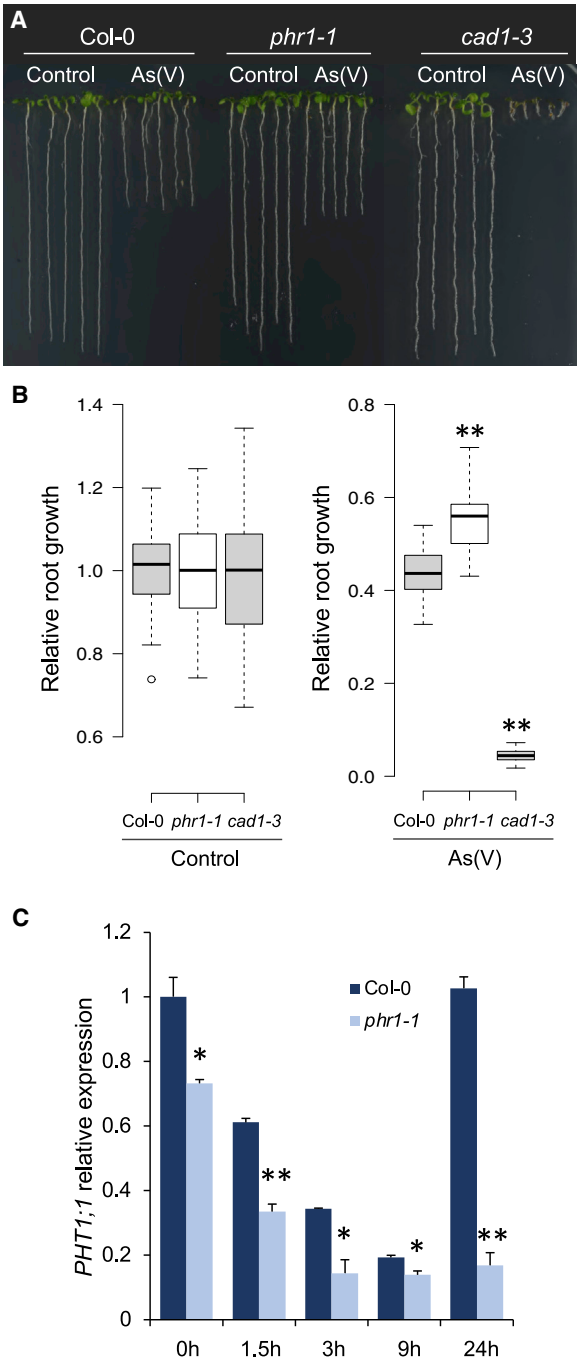

Figure 3. PHR1 modulates *PHT1;1* expression recovery.

(A) As(V) tolerance phenotypes of wild-type, *phr1-1* mutant, and *cad1-3* mutant plants grown in vertical agar plates containing 10 μM Pi Johnson medium supplemented with or without (control) 10 μM As(V) for 8 days. The figure is a representative sample of at least 40 plants analyzed in each case.

(B) The graphs show relative root growth quantification (ratio of primary root length of each individual in control or As(V) supplemented plates relative to the average primary root length of the corresponding genotype under control conditions) of wild-type, *phr1-1* mutant, and *cad1-3* mutant plants from the experiment shown in (A). Asterisks indicate significant differences from the wild type (ANOVA, $p < 0.001$).

(C) qRT-PCR analysis of *PHT1;1* expression in wild-type and *phr1-1* mutant plants. Plants were germinated on Johnson medium supplemented with 1 mM Pi in a horizontal position for 7 days and then transferred to Pi-free medium for 2 days. Plants were subsequently treated with 30 μM As(V). For the analysis, whole plants were collected at 0, 1.5, 3, 9, and 24 h after treatment. We used three independent biological replicates, each consisting of 15 plants. *$p < 0.05$, **$p < 0.01$ (Student's t test versus wild type). Error bars indicate SD.

to As(III) treatment using western blotting (Figure 2F). Confirming the confocal results, western blot analysis showed an initial reduction in PHT1;1 protein accumulation after As(III) treatment, followed by a recovery of PHT1;1 levels at 24 h (Figure 2F). These findings provide strong evidence that As(III) acts as an intracellular signal that allows plants to precisely adjust As(V) uptake to the activity of detoxification machinery.

Arsenate triggers PHR1 degradation to modulate PHT1;1 expression in response to arsenic

The transcription factor PHR1 is known to participate in the activation of *PHT1;1* under low Pi (Rubio et al., 2001; Bustos et al., 2010). Now, we wanted to investigate whether PHR1 activity was also involved in the regulation of *PHT1;1* in response to As(V). We first analyzed the As(V) tolerance phenotype of a *phr1-1* knockout (KO) mutant carrying a point mutation that leads to a premature stop codon and thus to a nonfunctional, truncated PHR1 protein (Rubio et al., 2001). To this end, we quantified the root length in wild-type and *phr1-1* plants with or without exposure to As(V). As a control, we also included the *cad1-3* mutant that exhibited a highly As(V) sensitive phenotype consistent with its lack of phytochelatins (Figure 3A and 3B). We found that *phr1-1* mutant plants displayed tolerance to As(V), as indicated by the significantly longer roots in *phr1-1* mutants relative to wild-type plants in the presence of As(V) (Figure 3A and 3B). This observation suggests that As(V) uptake may be compromised in the *phr1-1* mutant background. Accordingly, *PHT1;1* expression analysis showed that *PHT1;1* transcript accumulation was significantly lower in *phr1-1* plants (Figure 3C). As(V) efficiently repressed *PHT1;1* expression in the *phr1-1* mutant background, similar to its effect in wild-type plants. However, *PHT1;1* expression did not recover after 24 h of As(V) exposure according to a delay in As(V) uptake, suggesting that PHR1 may also be involved in coordinating *PHT1;1* transcript accumulation with the amount of arsenic.

Previous reports have shown that functional activation of PHR1 in response to Pi starvation does not depend on transcriptional regulation or changes in subcellular localization (Rubio et al., 2001). We therefore investigated whether As(V) regulates PHR1 stability. To this end, we used a transgenic line that expressed PHR1-GFP under the control of the PHR1 endogenous promoter in the *phr1-1* background (*pPHR1::PHR1-GFP*). Western blot analysis performed in these plants showed that As(V) triggers PHR1 degradation after 3 to 6 h of exposure (Figure 4A). Surprisingly, PHR1 stability was restored and its accumulation increased after 24 h when As(V) was already depleted from the medium (Figures 1B and 4A). In addition, the stability of unrelated transcription factors such as the brassinosteroid response regulator BES1 was not altered in response to As(V), indicating that PHR1 degradation was not a nonspecific effect of As(V) toxicity (Supplemental Figure 3). Also, PHR1 degradation was not observed in plants treated with Pi at the same concentration we used for As(V) (Figure 4A). Furthermore, treatment with the 26S proteasome inhibitor MG132 in

Please cite this article in press as: Navarro et al., Arsenite provides a selective signal that coordinates arsenate uptake and detoxification through the regulation of PHR1 stability in *Arabidopsis*, Molecular Plant (2021), https://doi.org/10.1016/j.molp.2021.05.020

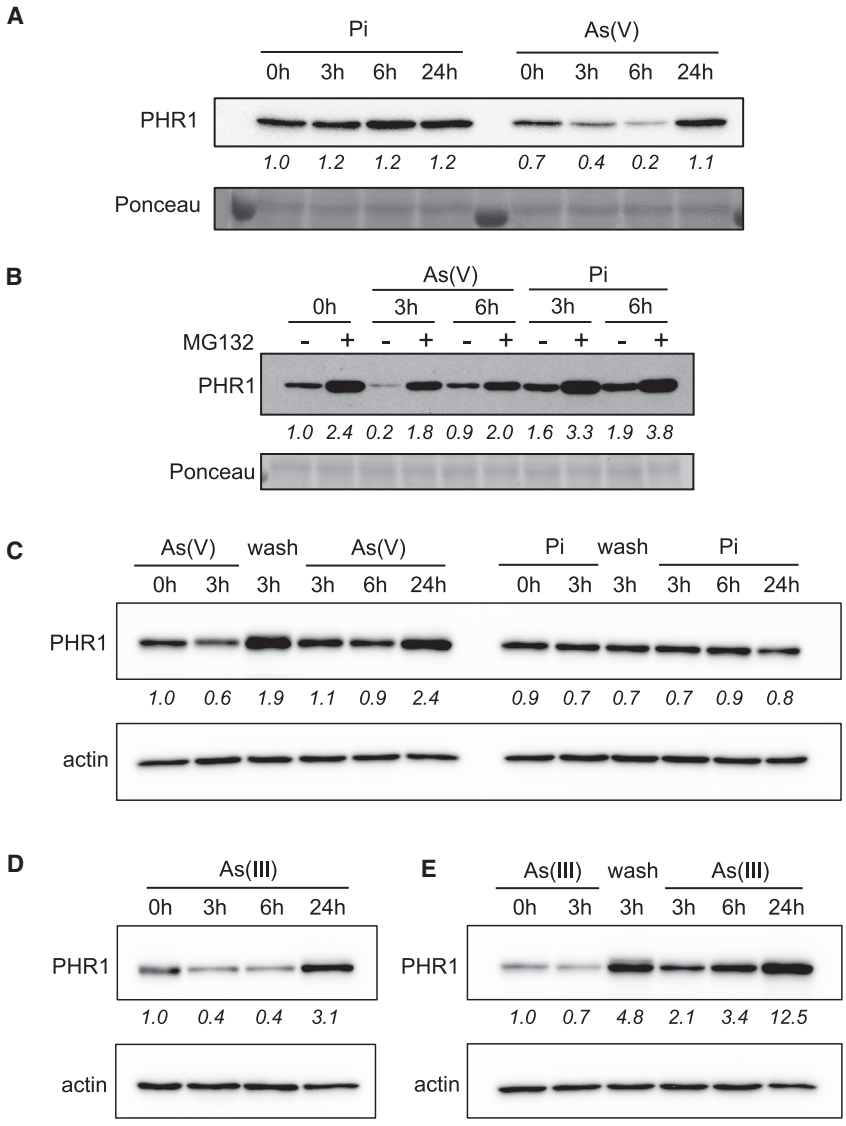

Figure 4. As(V) and As(III) trigger PHR1 degradation

(A) Immunoblot analyses of PHR1 protein levels in roots of *pPHR1::PHR1-GFP*-expressing plants. Plants were germinated on Johnson medium supplemented with 1 mM Pi in a horizontal position for 7 days and then transferred to low Pi for 2 days. Plants were subsequently treated with 30 μM Pi or 30 μM As(V). Root samples were collected 0, 3, 6, and 24 h after treatments. Ponceau S staining is shown as a loading control.

(B) PHR1 protein stability in the presence (+) or absence (−) of the proteasome inhibitor MG132. *pPHR1::PHR1-GFP*-expressing plants were grown in the conditions used in (A). Plants were pretreated with 50 μM MG132 for 2 h in Johnson-Pi liquid medium and subsequently treated with 30 μM Pi or 30 μM As(V) in the presence of 50 μM MG132. A control experiment without MG132 was conducted in parallel. Ponceau S staining is shown as a loading control.

(C) PHR1 protein degradation study using 35S::*HA*:*GR*:*PHR1* (Ox*PHR1*)-expressing plants. Plants were germinated on Johnson medium supplemented with 1 mM Pi in a horizontal position for 7 days and then transferred to Pi-free medium supplemented with 5 μM dexamethasone (DEX) for 2 days. The 5 μM DEX treatment was maintained until completion of the experiment. Plants were subsequently treated with 30 μM As(V) or 30 μM Pi (control condition) for 3 h and then washed with water for another 3 h. After this, plants were exposed again to 30 μM As(V) or 30 μM Pi for a maximum of 24 h. Root samples were collected before and after the first As(V)/Pi treatment, after the wash, and 3, 6, and 24 h after the second As(V)/Pi treatment. Actin levels are shown as a loading control.

(D) PHR1 protein degradation kinetics in Ox*PHR1*-expressing plants in response to 90 μM As(III). Plants were germinated and transferred as in (C) and then treated with 90 μM As(III). Actin levels are shown as a loading control.

(E) PHR1 protein degradation study using Ox*PHR1*-expressing plants grown in the conditions described in (C). In this case, plants were treated with 90 μM As(III) for 3 h and then washed with water for another 3 h. After this, plants were exposed again to 90 μM As(III) for a maximum of 24 h. Root samples were collected before and after the first As(III) treatment, after the wash, and 3, 6, and 24 h after the second As(III) treatment. Actin levels are shown as a loading control. In the figure, the numbers in italics below the lanes represent the adjusted relative band intensity expressed relative to the first lane of each gel and normalized to the corresponding loading control.

combination with As(V) abolished PHR1 degradation, supporting the notion that the ubiquitination-26S proteasome pathway is involved in PHR1 degradation in response to As(V) (Figure 4B).

Interestingly, we consistently found that the amount of PHR1 accumulated in the recovery phase after As(V) treatment was higher than that observed in plants that were not exposed to the metalloid (Figure 4A and 4B). This observation suggests that As(V) exposure promotes enhanced PHR1 accumulation during re-stabilization. Although *PHR1* transcript accumulation is not altered in response to Pi starvation (Rubio et al., 2001), it has been previously reported that *PHR1* can be transcriptionally regulated by environmental factors like light (Liu et al., 2017). We therefore decided to analyze whether *PHR1* transcriptional regulation could be responsible for the variations in PHR1 stability. qRT-PCR analysis in the *pPHR1::PHR1-GFP* line showed that *PHR1* transcript accumulation was not altered after 3 h of As(V) treatment, and there was a slight but significant increase after 6 h (Supplemental Figure 4), corresponding to the maximum *PHT1;1* repression (Figure 3C) and minimum PHR1 accumulation (Figure 4A). We also observed a significant increase in *PHR1* transcript accumulation after 24 h of As(V) exposure, which may explain at least in part the observed PHR1 protein hyperaccumulation.

To further assess the role of transcriptional regulation in the recovery of PHR1 stability in response to As(V), we determined PHR1 protein levels in transgenic HA-tagged *PHR1*-overexpressing (Ox*PHR1*) lines under the control of a constitutive promoter. Thus, in these lines, the transcriptional regulation in response to arsenic is overridden (Bustos et al., 2010). As shown in Supplemental Figure 5A, the Ox*PHR1* line perfectly mimics the

Please cite this article in press as: Navarro et al., Arsenite provides a selective signal that coordinates arsenate uptake and detoxification through the regulation of PHR1 stability in *Arabidopsis*, Molecular Plant (2021), https://doi.org/10.1016/j.molp.2021.05.020

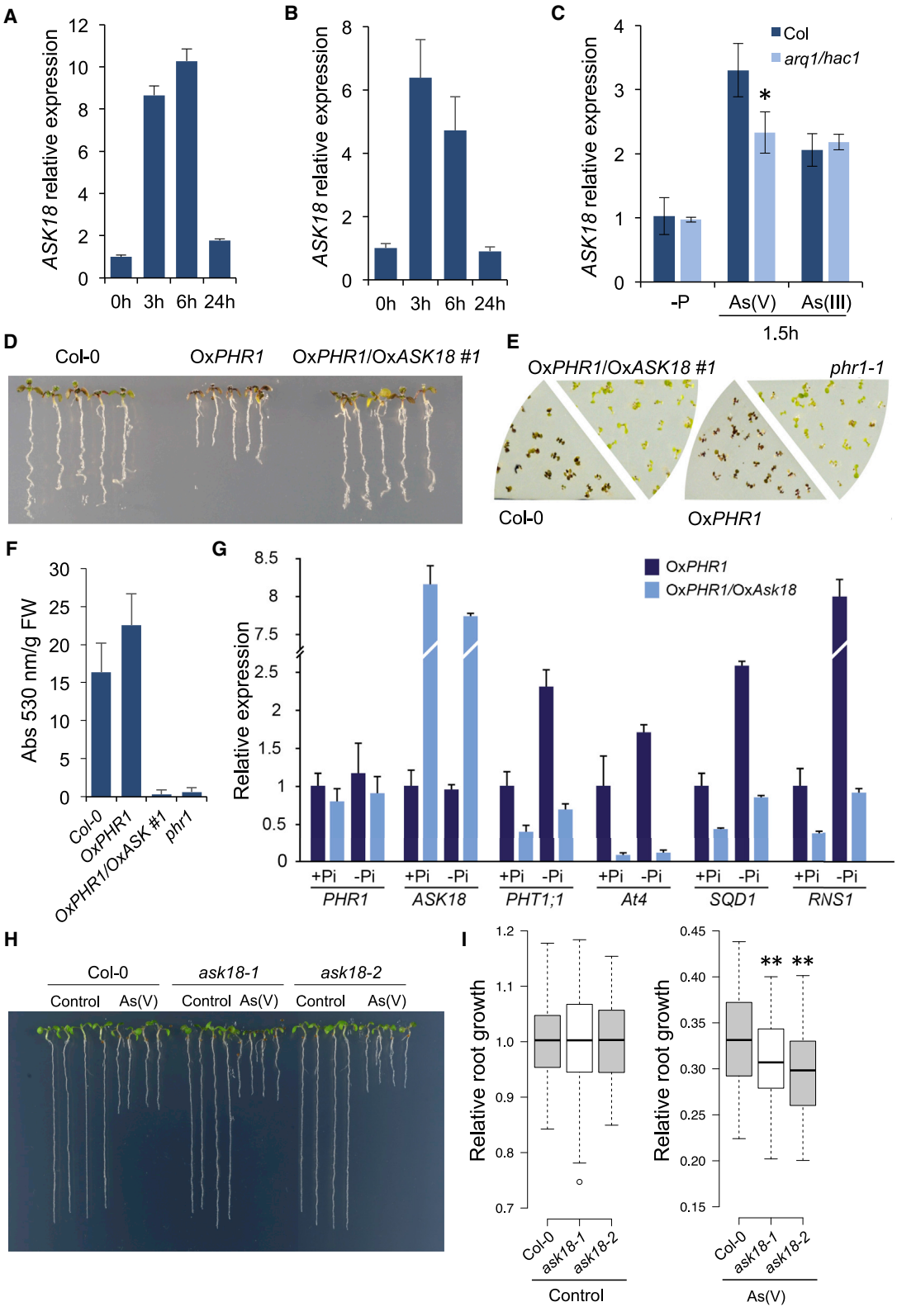

Figure 5. Arsenic-inducible *ASK18* is a regulator of PHR1 stability.

(A and B) qRT-PCR analysis of *ASK18* kinetic expression in response to As(V) (A) or As(III) (B). Wild-type plants were germinated on Johnson medium supplemented with 1 mM Pi in a horizontal position for 7 days and then transferred to Pi-free medium for 2 days. Plants were subsequently treated with 30 μM As(V) or 60 μM As(III) in liquid conditions. Gene expression was analyzed in whole plants collected 0, 3, 6, and 24 h after treatments.

(legend continued on next page)

Please cite this article in press as: Navarro et al., Arsenite provides a selective signal that coordinates arsenate uptake and detoxification through the regulation of PHR1 stability in *Arabidopsis*, Molecular Plant (2021), https://doi.org/10.1016/j.molp.2021.05.020

pPHR1::PHR1-GFP line in terms of PHR1 degradation and subsequent enhanced recovery after As(V) exposure. We also found that the initial repression of *PHT1;1* expression after As(V) exposure and its subsequent increased accumulation were similar to those observed in the *pPHR1::PHR1-GFP* lines (Supplemental Figure 5B). Therefore, we concluded that *PHR1* transcriptional regulation is not a primary factor in PHR1 hyperaccumulation. Importantly, we linked the stability of PHR1 to the level of As(V) in the medium. Increased PHR1 accumulation was also observed when As(V) was washed after 3 h of As(V) treatment, and PHR1 degradation was observed when plants were reexposed to As(V) (Figure 4C). Taken together, all these observations indicate that plants are able to efficiently respond to As(V) levels by modulating PHR1 accumulation, and this coordination may be regulated by the effective levels of nonsequestered As(III).

Next, we studied the effect of As(III) on PHR1 stability. We exposed the *OxPHR1* line to 90 μM As(III) and quantified the level of PHR1 accumulation by western blotting. Similar to As(V), treatment with As(III) triggers rapid PHR1 degradation followed by the accumulation of PHR1 after 24 h (Figure 4D). Accordingly, As(III) removal by washing restored PHR1 protein levels, and subsequent As(III) exposure led again to PHR1 degradation (Figure 4E). Next, we explored whether high Pi levels could override the As(III) signal. Under high Pi, the expression of *PHT1;1* and its localization in the membrane is marginal, therefore, under these conditions, the activation of the arsenic response relies on As(III) uptake through aquaporins (NIPs) (Zhao et al., 2009). First, we asked whether under sufficient Pi conditions, when the low Pi response is off, As(III) alone is able to regulate the degradation of PHR1. We analyzed the degradation of PHR1 in response to As(III) in the presence of a gradient of Pi concentrations (0, 100 μM, 500 μM, and 1000 μM Pi) at 6 h and 24 h. In all cases, we observed the typical rapid degradation of PHR1 at 6 h (Supplemental Figure 6A) and its subsequent recovery after 24 h (Supplemental Figure 6B). We demonstrated that the differences in PHR1 stability were not caused by changes in the level of PHR1 expression (Supplemental Figure 6C). We also observed the typical rapid induction of *ASK18* and *WRKY6* and the repression of *PHT1;1* in response to As(III) in plants grown under a gradient of Pi (Supplemental Figure 6D–6F). We concluded that the lack of activation of the PSR under high Pi conditions does not interfere with the activation of arsenic signaling by As(III). These results further support the idea that As(III) is the main signal that regulates the repression and restoration of *PHT1;1* expression through transitory changes in PHR1 stability and *WRKY6* expression.

Identification of the molecular components involved in PHR1 degradation

To identify molecular components involved in PHR1 degradation in response to As(III) signaling, we searched for As(V)-responsive genes that encoded components of the ubiquitination-26S proteasome machinery. To this end, we first performed Gene Ontology (GO) analysis on a transcriptomic dataset of plants exposed to As(V) for 1.5 and 8 h that had been previously generated in our laboratory (Castrillo et al., 2013). GO analysis using the GO term annotation tool from TAIR (https://www.arabidopsis.org/tools/bulk/go/index.jsp) identified 18 As(V)-responsive transcripts annotated with the GO term "ubiquitin-dependent protein catabolic process" (GO:0006511) (Supplemental Figure 7A). Interestingly, only one gene, *AT1G10230*, encoding an SKP1-like 18 protein (ASK18), was induced after 1, 5, and 8 h of As(V) exposure, matching the PHR1 degradation kinetics (Figure 4A). SKP1-like proteins are subunits of the SCF complex, the most important family of ubiquitin protein ligases that control the stability of signal transducers and transcriptional regulators in a wide variety of biological processes (Chen and Hellmann, 2013; Ban and Estelle, 2021). These proteins link Cullin with F-Box proteins that interact with their substrates, taking them to the 26S proteasome for specific degradation (Zheng et al., 2002).

The expression kinetics of *ASK18* in response to As(V) was measured by qRT-PCR expression analysis in plants exposed to the metalloid (Figure 5A). This experiment enabled us to confirm that *ASK18* is transiently induced by As(V), reaching maximum expression after 6 h of As(V) treatment and then gradually diminishing to basal levels at 24 h of exposure, when As(V) is practically absent from the media (Figures 1B and 5A). These expression kinetics of *ASK18* transcript accumulation were in perfect accord with the kinetics of PHR1 accumulation in response to As(V), and both were opposite to those observed in *PHT1;1*. In accordance with our previous observations, transcript accumulation analysis performed in plants exposed

(C) *ASK18* expression in wild-type and *arq1/hac1* mutant plants treated with 20 μM As(V) or 30 μM As(III). Plants were grown as in (A) and then treated with 20 μM As(V) or 30 μM As(III) for 1.5 h. Gene expression was analyzed in whole plants collected 0 and 1.5 h after treatments. *$p < 0.05$ (Student's t test versus the wild type).

(D) As(V) tolerance phenotype of wild-type (Col-0), Ox*PHR1*, and double over-expressor Ox*PHR1*/Ox*ASK18* line #1 plants grown on Johnson medium containing 7.5 μM Pi and 15 μM As(V) supplemented with 5 μM DEX for 10 days.

(E) Anthocyanin accumulation in plants of the wild type (Col-0), Ox*PHR1* line, Ox*PHR1*/Ox*ASK18* line #1, and *phr1-1* mutant grown in phosphate-free medium plates in the presence of 5 μM DEX.

(F) Anthocyanin quantification in plants from (E). In each case, the absorbance at 530 nm was normalized by the fresh weight (FW) of the samples (Abs 530 nm/g FW). We used three independent replicates per genotype, each consisting of at least 15 plants.

(G) qRT-PCR analysis of PHR1 target genes in Ox*PHR1* and Ox*PHR1*/Ox*ASK18* lines. Plants were grown on Johnson medium supplemented with 1 mM Pi for 7 days and then transferred to phosphate-free (−Pi) or 1 mM Pi (+Pi) medium supplemented with 5 μM DEX for 3 days.

(H) Phenotypic analysis of wild-type plants and two independent *ASK18* T-DNA insertion lines (*ask18-1* and *ask18-2*) in response to As(V) treatment. Plants were grown in vertical plates that contained 10 μM Pi alone (control) or in combination with 10 μM As(V) for 8 days.

(I) Relative root growth quantification (ratio of primary root length of each individual in control or As(V) supplemented plates to the average primary root length of the corresponding genotype under control conditions) of wild-type and *ask18* mutant plants from the experiment shown in (H). The quantification was performed using at least 32 plants in each case. Error bars indicate SD. **$p < 0.005$ (Student's t test versus the wild type). For all qRT-PCR experiments, a total of three biological replicates were used, each consisting of 15 plants.

Please cite this article in press as: Navarro et al., Arsenite provides a selective signal that coordinates arsenate uptake and detoxification through the regulation of PHR1 stability in *Arabidopsis*, Molecular Plant (2021), https://doi.org/10.1016/j.molp.2021.05.020

to As(III) showed that *ASK18* was induced with a pattern similar to that observed in response to As(V) (Figure 5B). Furthermore, *ASK18* expression was lower in the *arq1/hac1* mutant, which accumulates less As(III) than wild-type plants (Figure 5C). This result further underlines the importance of As(III) as a signaling molecule that regulates As(V) uptake.

We next determined the subcellular localization of ASK18 by transient expression of a GFP-tagged version of ASK18 in *Nicotiana benthamiana* (*N. benthamiana*) leaves. As shown in Supplemental Figure 7B, ASK18 was observed in the cytoplasm and nuclei, overlapping with the localization of PHR1 (Rubio et al., 2001).

To examine whether ASK18 is involved in As(V)-mediated PHR1 degradation, we first obtained *Arabidopsis* lines that overexpressed *ASK18* in a transgenic background line that also overexpressed a functional tagged version of PHR1 (*OxASK18/OxPHR1*) (Bustos et al., 2010). As shown in Supplemental Figure 8A, the *OxASK18/OxPHR1* transgenic lines displayed remarkably enhanced PHR1 degradation. In line with this observation, *ASK18* overexpression fully complemented the As(V)-sensitive phenotype caused by *PHR1* overexpression (Figure 5D and Supplemental Figure 8B and 8C). We also analyzed anthocyanin accumulation, a classical response to Pi starvation that is tightly regulated by PHR1 (Rubio et al., 2001). Anthocyanin quantification experiments showed that *OxASK18/OxPHR1* plants were impaired in anthocyanin accumulation (Figure 5E and 5F, and Supplemental Figure 8D and 8E), mimicking the *phr1-1* mutant. Furthermore, we performed qRT-PCR expression analysis of a set of Pi-starvation responsive genes in *OxASK18/OxPHR1* lines (Figure 5G). The Pi-starvation inducible genes *PHT1;1*, *At4*, *SQD1,* and *RNS1* showed lower transcript accumulation in *OxASK18/OxPHR1* lines than in the parental line *OxPHR1*. This effect was exacerbated when plants were transferred to low Pi medium for 3 days (Figure 5G). Finally, we determined the As(V) tolerance phenotype of *ask18* transfer DNA (T-DNA) insertion mutants with reduced expression of *ASK18* (Supplemental Figure 8F and 8G). As shown in Figure 5H, *ask18* T-DNA null mutants exhibited an As(V)-sensitive phenotype relative to the wild-type plants. Quantification of root length confirmed that roots were significantly shorter in *ask18 mutants* than in wild-type plants (Figure 5I), consistent with increased PHR1 stability. All these findings are consistent with a role of ASK18 in PHR1 degradation.

To identify additional components that determine PHR1 degradation, we searched for ASK18 interactors in the Bio-Analytic Resource (BAR) database (Geisler-Lee et al., 2007; Dong et al., 2019) at http://bar.utoronto.ca/interactions2. Among all the interactors found (Supplemental Table 1), seven were experimentally determined proteins in the BioGRID, Intact, and PPI-BAR databases (Supplemental Figure 9A), and six of them encoded F-box proteins (Supplemental Figure 9B). We checked the interaction of the F-box proteins with ASK18 using the yeast two-hybrid assay (Y2H). Using ASK18 as prey and the six F-boxes as baits, we confirmed that two of them, AT5G49610 and AT3G61590, interacted with ASK18 (Figure 6A, left panel). Moreover, using ASK18 as bait, we again observed the interaction of AT3G61590 and found that AT5G49000 also interacted with ASK18 (Figure 6A, right panel). We then performed additional Y2H experiments with these three F-box proteins using PHR1 as bait or prey (Figure 6B). These experiments showed that one F-box protein, AT5G49000, consistently interacted with PHR1. We therefore named AT5G49000 PHR1 Interactor F-box1 (PHIF1). To confirm the interaction of PHIF1 with PHR1, we carried out *in vivo* and semi-*in vivo* experiments. First, we performed semi-*in vivo* pull-down assays using recombinant PHIF1 fused with MBP and extracts of transgenic plants overexpressing an HA-tagged version of PHR1 (Ox*PHR1*). As shown in Figure 6C, MBP-PHIF1 bound to PHR1 using extracts of plants treated with or without As(V). The amount of PHR1 in As(V)-treated plants was lower than that in untreated plants, in line with the observed PHR1 degradation in response to the metalloid. Finally, a co-immunoprecipitation assay was performed using *N. benthamiana* leaves co-transfected with HA-PHR1 and GFP-tagged PHIF1 (Figure 6D). The results showed that PHR1 co-immunoprecipitated with the F-box.

Next, we performed *in vivo* assays to test whether PHIF1 promoted degradation of PHR1. Transient co-expression assays of PHR1 and PHIF1 tagged versions showed that PHIF1 co-expression led to enhanced PHR1 degradation (Figure 7A). We consistently obtained identical results with the untagged version of PHIF1 (Supplemental Figure 10). In addition, we performed PCR analysis in two *phif1* KO T-DNA insertion lines that we named *phif1-1* and *phif1-2*. Both mutant alleles behaved as null, with no detectable transcript accumulation (Supplemental Figure 11A and 11B). Consistent with enhanced PHR1 stability, basal levels of *PHT1;1* transcripts in these mutants were significantly higher in both *phif1* background alleles compared with those observed in the wild-type plants (Figure 7B; Supplemental Figure 11C). In line with increased PHR1 stability in both *phif1* alleles, we observed higher Pi accumulation in the mutants than in the wild-type plants (Supplemental Figure 12). Furthermore, arsenic quantification of *phif1* mutant plants exposed to As(V) showed that both lines accumulated significantly higher amounts of arsenic than wild-type plants (Figure 7C; Supplemental Figure 11D).

To further confirm the role of PHIF1 in PHR1 degradation, we analyzed the As(V) tolerance of both *phif1* T-DNA insertion mutants. Phenotypic analysis showed that *phif1* exposed to As(V) exhibited an As(V)-sensitive phenotype (Figure 7D; Supplemental Figure 11E). *phif1* roots were significantly shorter than those of wild-type plants (Figure 7E; Supplemental Figure 11F), consistent with increased PHR1 stability. All of these observations allowed us to conclude that ASK18 and PHIF1 are key regulatory factors that control PHR1 degradation in response to arsenic.

DISCUSSION

Plants must cope with diverse abiotic stresses, including nutrient deficiency and heavy metal toxicity, that have detrimental effects on plant growth and development, productivity, and/or public health. The problem of nutrient deficiency and heavy metal toxicity is particularly relevant when the nutrient and the toxic element are similar and use the same uptake systems, as is the case for Pi and As(V). The mechanisms that allow plants to deal with As(V) without compromising Pi acquisition remain largely unknown. Here we show that As(III) regulates

Please cite this article in press as: Navarro et al., Arsenite provides a selective signal that coordinates arsenate uptake and detoxification through the regulation of PHR1 stability in *Arabidopsis*, Molecular Plant (2021), https://doi.org/10.1016/j.molp.2021.05.020

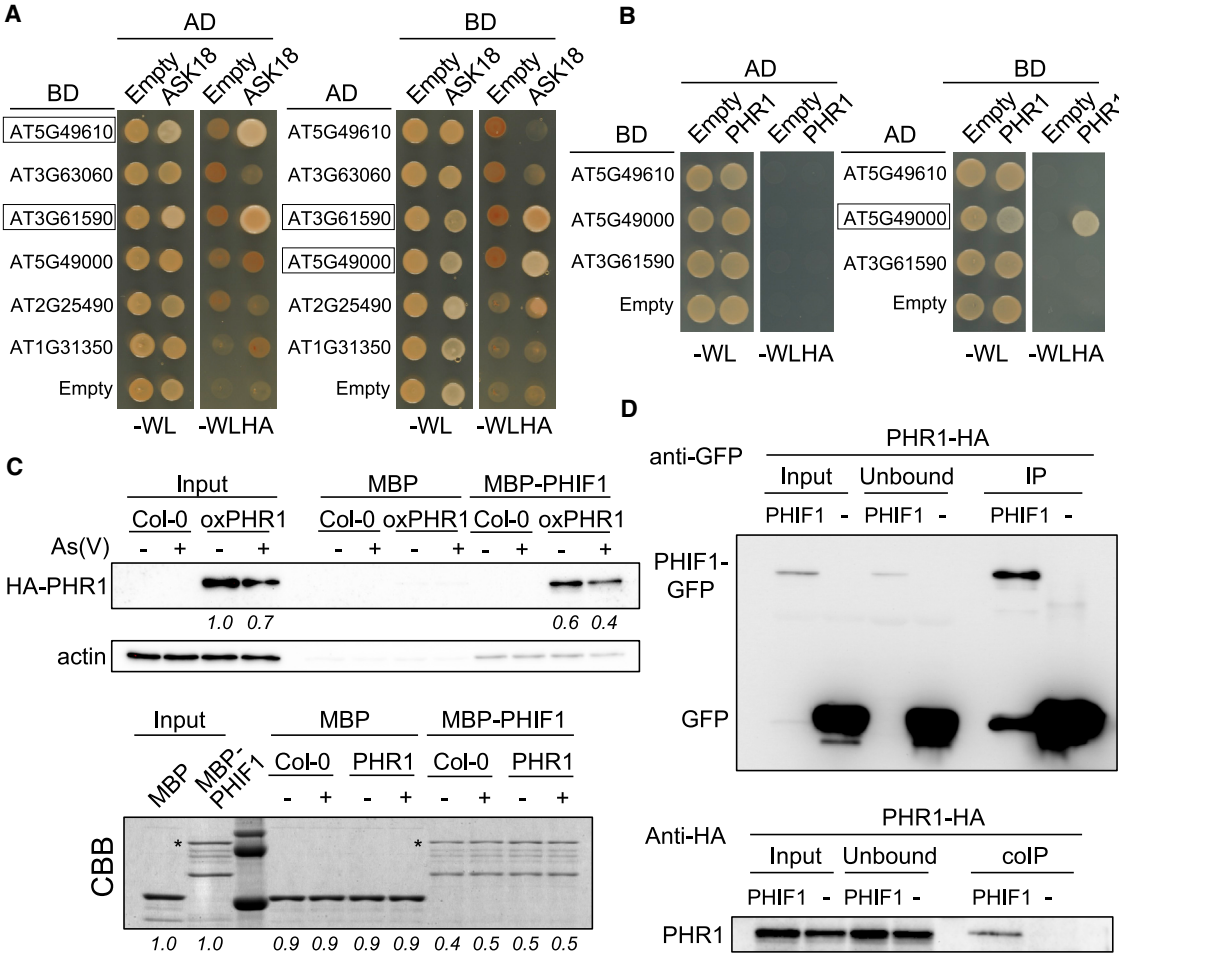

Figure 6. ASK18 and PHR1 interact with F-box proteins.

(A and B) Yeast two-hybrid assay for ASK18 (A) and PHR1 (B) with the candidate F-box interacting proteins. In each case, ASK18 and PHR1 proteins were used as prey (left) or as bait (right). AD, activation domain; BD, binding domain; –WL, SD minimal medium lacking tryptophan and leucine; –WLHA, SD minimal medium lacking tryptophan, leucine, histidine, and alanine. F-boxes that interact with ASK18 and PHR1 in (A) and (B) are highlighted by a square. In all cases, the empty vector was used as a control.

(C) Semi-*in vivo* pull-down analysis of the PHIF1-PHR1 interaction. Wild-type (Col-0) and *HA*:*GR*:*PHR1* (Ox*PHR1*) overexpressing plants were grown on J+P (1 mM Pi) plates, transferred to Pi-free medium for 2 days, and then treated (+) or not (–) with 30 μM As(V) in liquid Pi-free medium for 2 h. Equal amounts of root protein extracts from these plants were incubated with *in vitro* purified MBP-PHIF1 and MBP (control) bound to amylose resin. The upper panel shows immunoblot hybridization with anti-HA, detecting HA-PHR1 fusion protein in the input or in the pulled-down eluate. Actin levels are shown as a loading control. The lower panel shows the input MBP-tagged proteins used as bait and 1/10 of the pulled-down eluate stained with Coomassie Brilliant Blue (CBB). Asterisks indicate the PHIF1 full-length protein. The numbers in italics below the lanes represent the adjusted relative band intensity, expressed relative to the first input lane and normalized to the corresponding actin loading control. Intensity of the Coomassie-stained proteins was expressed relative to that of the corresponding input protein.

(D) Co-immunoprecipitation analysis of PHR1 with the F-box protein PHIF1. HA-PHR1 was transiently expressed in combination with PHIF1-GFP or GFP alone in *N. benthamiana* leaves. Protein extracts were immunoprecipitated (IP) with anti-GFP antibody (upper panel), and the co-immunoprecipitated (coIP) interacting proteins were detected with anti-HA antibody (lower panel).

the expression of As(V)/Pi transporters, providing a highly selective signal to adapt As(V) uptake to the arsenic detoxification machinery. In addition, we uncover a regulatory mechanism that limits As(V) uptake based on the As(III)-mediated degradation of PHR1, and we identify two components of the ubiquitination machinery: a highly As(III)-responsive gene encoding a SKP1-like protein (ASK18) and a specific PHR1-interacting F-box (PHIF1) involved in PHR1 degradation.

In nature, wild plants limit As(V) uptake as the main strategy to tolerate As(V) by suppression/repression of PHT1 transporters (Meharg and Macnair, 1990, 1991; Bleeker et al., 2003). Repression of Pi transporters has also been reported in *Arabidopsis* and in crop species (Misson et al., 2004; Castrillo et al., 2013; Kamiya et al., 2013; Puga et al., 2014; Zvobgo et al., 2018). Therefore, plants broadly respond to the presence of As(V) in a coordinated manner to interrupt the whole Pi/As(V) uptake system, compromising Pi uptake. Here we found that *PHT1;1* expression is restored once arsenic disappears from the medium and is present exclusively in plant tissue, probably sequestered in the vacuole. Similar results were obtained with *PHO1*, the Pi transporter involved in xylem loading (Hamburger

Please cite this article in press as: Navarro et al., Arsenite provides a selective signal that coordinates arsenate uptake and detoxification through the regulation of PHR1 stability in *Arabidopsis*, Molecular Plant (2021), https://doi.org/10.1016/j.molp.2021.05.020

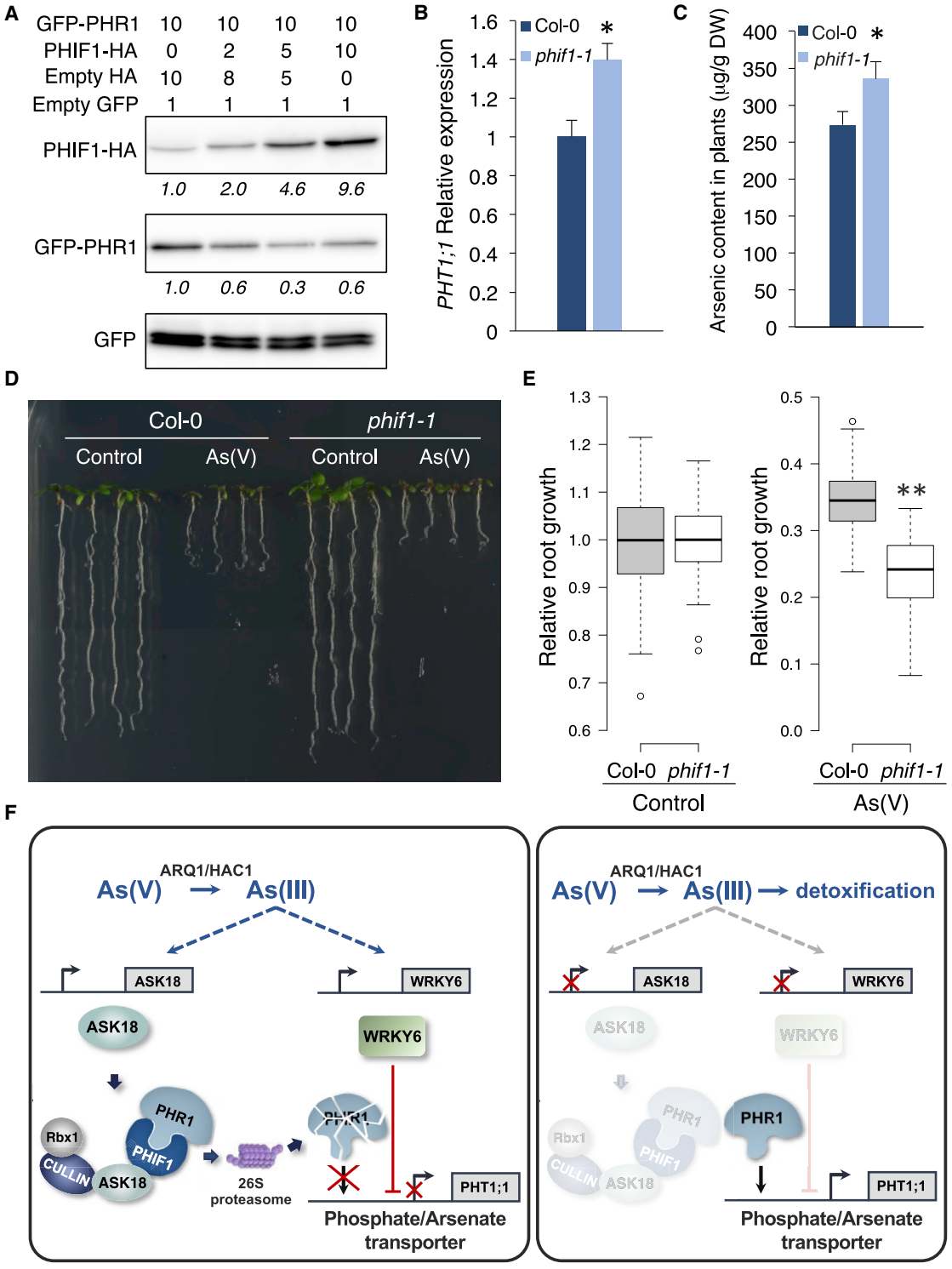

Figure 7. F-box protein PHIF1 mediates PHR1 degradation in response to arsenic.

(A) *In vivo* degradation assay of PHR1 by PHIF1 in *N. benthamiana* leaves. GFP1-PHR1 was transiently co-expressed with increasing amounts of PHIF1-HA. GFP alone was used as a control. Relative amounts of each construct are indicated by numbers above the blots. Protein extracts were immunoblotted against anti-HA and anti-GFP antibodies. The numbers in italics below the lanes represent the adjusted relative intensity expressed relative to the first input lane and normalized to the corresponding GFP loading control.

(B) qRT-PCR analysis of *PHT1;1* expression in wild-type plants (Col-0) and *phif1-1* mutants grown in horizontal agar plates with Johnson medium supplemented with 1 mM Pi for 7 days and then transferred to Pi-free medium for 2 days. For this analysis, whole plants from three independent biological replicates were used, each consisting of 15 plants. *$p < 0.05$ (Student's t test versus the wild type).

(legend continued on next page)

Please cite this article in press as: Navarro et al., Arsenite provides a selective signal that coordinates arsenate uptake and detoxification through the regulation of PHR1 stability in *Arabidopsis*, Molecular Plant (2021), https://doi.org/10.1016/j.molp.2021.05.020

et al., 2002). This observation suggests that repression and expression recovery of Pi transporters is tightly modulated by the detoxification machinery. Indeed, arsenic speciation analysis performed here showed that As(V) is quickly reduced to As(III), the main chemical form that plants handle to sequester arsenic in vacuoles. The *cad1-3* mutant, altered in phytochelatin biosynthesis and therefore impaired in arsenic sequestration, did not restore *PHT1;1* expression. In fact, As(III) is equally distributed in the medium and in the plant tissue of this mutant, suggesting that most As(III) is located free in the cytoplasm. In line with a previous publication (Liu et al., 2010), we showed that the *cad1-3* mutant is extremely sensitive to arsenic, suggesting that, consistent with previous observations (Liu et al., 2010), As(III) complexation with phytochelatins is an important factor for arsenic tolerance in *Arabidopsis*. Furthermore, the delay observed in the recovery of *PHT1;1* expression in response to arsenic in *cad1-3* highlights the importance of As(III) sequestration in the control of *PHT1;1* expression. Accordingly, weak mutant alleles of *PHT1;1*, which exhibited diminished As(V) uptake, showed increased arsenic content compared with wild-type plants (Catarecha et al., 2007). All these observations indicate that plants coordinate As(V) uptake with the accumulation rate of As(III) in the vacuole as a basic requirement for arsenic tolerance.

In this study, we discovered that *WRKY6* and *ASK18* expression and PHR1 degradation are tightly regulated by As(III). Because these regulators are not involved in As(III) detoxification, we speculated that this chemical species could be the main signal of arsenic response in plants. To support this idea, we showed that the *arq1/hac1* mutant, impaired in the reduction of As(V) to As(III), displays reduced responsiveness of *WRKY6* and *ASK18*. Furthermore, confocal microscopy and analysis of PHT1;1 protein levels performed in plants exposed to As(III) suggested that *PHT1;1* transcriptional repression in response to As(III) leads to PHT1;1 delocalization from the plasma membrane and transport through the endocytic pathway for turnover in the vacuole. Once As(III) is sequestered, *PHT1;1* expression recovery leads to PHT1;1 reaccumulation and relocation in the membrane. This mechanism allows plants to adapt As(V) uptake to detoxification processes.

It has been suggested that billions of years ago, when oxygen was scarce, As(III) would have been the prominent chemical species of arsenic. This leads us to speculate that As(III) was an important selective force driving the evolution of As(III) sequestration and extrusion strategies in plants. Once oxygen increased, As(V) became the prevalent chemical form (Zhu et al., 2014), and organisms evolved As(V) extrusion/sequestration mechanisms (Chen et al., 2016; Cai et al., 2019) or were forced to recruit As(V) reductases to rapidly reduce As(V) to As(III) (Mukhopadhyay and Rosen 2002; Chen et al., 2020). It is not surprising that an ancestral molecule such as As(III) controls the expression and stability of As(V)/Pi transporters, their localization in the membrane, and the degradation of PHR1. This new sensing mechanism efficiently adapts arsenate uptake to the As(III) accumulation rate in the vacuole.

In this work, we reveal that PHR1, the master transcriptional activator of the PSR (Rubio et al., 2001; Zhou et al., 2008; Ren et al., 2012; Wang et al., 2013a, 2013b, 2019; Xue et al., 2017), is also involved in the arsenic response. PHR1 is an essential component for the activation of the high-affinity *PHT1* Pi transporters in *Arabidopsis*, including *PHT1;1* and *PHT1;4*, which are also responsible for As(V) uptake (Shin et al., 2004; Catarecha et al., 2007). Here, we found that As(V) repression of *PHT1;1* and *PHO1* co-occurs with PHR1 degradation as an additional control mechanism to prevent As(V) uptake. In line with the observed *PHT1;1* expression recovery when As(V) is removed from the medium, PHR1 stability was also quickly restored, allowing plants to recover Pi uptake once arsenic was fully extruded or sequestered in the vacuole. The transient degradation of PHR1 represents a new regulatory layer that controls PHT1;1 activity. Previously in our lab, we found that *PHT1;1* repression by As(V) is mediated by the transcription factor WRKY6 (Castrillo et al., 2013). Interestingly, this regulator is also involved in the repression of the Pi transporter *PHO1* in response to Pi sufficient conditions (Chen et al., 2009). Here, we found that these two regulatory layers are coordinated but represent independent regulatory pathways. Supporting this conclusion, we found that the repression rate of *PHT1;1* in the *phr1-1* background is similar to that observed in wild-type plants, indicating that WRKY6 is able to repress *PHT1;1* in the absence of PHR1, excluding an essential role of PHR1 in the repression of *PHT1;1*. However, *PHT1;1* is not able to recover its expression in the *phr1-1* background, reinforcing the role of PHR1 as an inducer of *PHT1;1* during the recovery phase. Therefore, strict coordination between the activator PHR1 and the repressor WRKY6 is needed to coordinate PHT1;1 activity in response to arsenic. Such control may exist for other members of the PHT1 family such as PHT1;4, whose expression in response to Pi and arsenic is similar to that of PHT1;1.

(C) Total arsenic quantification in whole plants from wild-type (Col-0) and *phif1-1* mutants. Plants were grown on Johnson medium supplemented with 1 mM Pi in a vertical position for 7 days, transferred to Pi-free conditions for 2 days, and then exposed to 30 μM As(V) in liquid conditions for 6 h. For this analysis, three independent biological replicates were used, each consisting of at least 100 plants. *$p < 0.05$ (Student's t test versus the wild type).
(D) As(V) tolerance of wild-type and *phif1-1* mutant plants. Plants were grown in horizontal plates containing 10 μM Pi alone (control) or in combination with 15 μM As(V) for 8 days.
(E) Relative root growth quantification (ratio of primary root length of each individual in control or As(V) supplemented plates to the average primary root length of the corresponding genotype under control conditions) of wild-type and *phif1-1* mutant plants from the experiment shown in (D). At least 49 plants were analyzed in each case. **$p < 0.001$ (Student's t test versus the wild type).
(F) A proposed model for arsenic response in *Arabidopsis* roots. In low phosphate conditions (control conditions), the high-affinity Pi/As(V) transporter *PHT1;1* is actively transcribed. Upon As(V) exposure, the metalloid enters the cell through *PHT1;1* transporters. As(V) is rapidly reduced to As(III) by the action of the arsenate reductase ARQ1/HAC1. As(III) signaling modulates the major regulators of *PHT1;1* by inducing the transcription of *WRKY6* (a *PHT1;1* repressor) and *ASK18* (a component of the SCF complex that interacts with the F-box protein PHIF1). PHIF1 targets the *PHT1;1* activator, PHR1, for protein degradation. As a result of these coordinated events, *PHT1;1* expression is repressed, and As(V) uptake is reduced. As(III) is internalized into the vacuoles as As(V) is progressively removed from the medium. When the external concentration of the metalloid reaches low levels, *PHT1;1* expression is restored, and root cells recover Pi acquisition capacity. The use of arsenite as a signal provides a selective mode to coordinate As(V) uptake with the arsenic detoxification capacity. Error bars indicate SD.

Please cite this article in press as: Navarro et al., Arsenite provides a selective signal that coordinates arsenate uptake and detoxification through the regulation of PHR1 stability in *Arabidopsis*, Molecular Plant (2021), https://doi.org/10.1016/j.molp.2021.05.020

Control of protein stability through ubiquitination is a flexible and rapid response that contributes to plant adaptation to a multitude of environmental stresses (Kurepa et al., 2009; Lee and Kim, 2011; Lyzenga and Stone, 2012; Stone, 2014; Cho et al., 2017; Xu and Xue, 2019). Multiple reports have shown that several regulators of the PSR, including PHR1 interactors and WRKY6, are subjected to posttranslational modifications such as sumoylation of PHR1 (Miura et al., 2005) or ubiquitination of SPX proteins and Pi transporters (Bayle et al., 2011; Lv et al., 2014; Puga et al., 2017; Yang et al., 2018; Hu et al., 2019; Medici et al., 2019; Ruan et al., 2019; reviewed in Pan et al., 2019). In relation to As(V), components of the 26S proteasome complex in rice and *Arabidopsis* are involved in the degradation of arsenic transporters (Lim et al., 2014), the regulation of genes involved in phytochelatin biosynthesis (Sung et al., 2009), and enhanced growth in the presence of arsenic (Hwang et al., 2016, 2017). However, the role of ubiquitination in the arsenic response remains mostly unknown. In this work, we identified constituents of the ubiquitin E3 ligase complex responsible for PHR1 degradation. Looking for As(V)-responsive components of the ubiquitin-proteasome machinery, we identified ASK18, an SKP1-like protein involved in the assembly of the SCF ubiquitin ligase complex. In addition, searching for F-box proteins that interact with ASK18 enabled us to identify the F-box PHIF1 that interacts with PHR1. Experimental evidence provided here indicates that PHIF1 is involved in PHR1 degradation in response to As(III). In general, F-box proteins are responsible for selecting proteolytic substrates, whereas SKP1 proteins are considered to act as scaffolds that bridge cullin and F-box proteins to assemble the SCF complex. However, SKP1-like proteins exhibit a wide spectrum of expression patterns (Zhao et al., 2003; Dezfulian et al., 2012), and here we have shown that ASK18 is highly responsive to As(III), providing further control of PHR1 in addition to its selective interaction with PHIF1. This level of specificity conferred by ASK18, expressed only in response to arsenic, is critical for the control of other regulatory elements relevant to the degradation of PHR1 that may be shared between low Pi and As responses, such as PHIF1. *phif1* alleles promote significant *PHT1;1* transcript accumulation under low Pi conditions and increased Pi accumulation in response to Pi supply, suggesting that PHIF1 may have a role in Pi uptake. We speculate that in addition to PHIF1, other overlapping components between the arsenic and Pi signaling pathways may exist in the PHR1 degradation complex. Similar control of specificity has been observed in the control of WRKY6, which has a dual function as a repressor in both the arsenic and Pi signaling pathways. Although the regulation of WRKY6 protein stability in response to arsenic remains unknown, it has been reported that WRKY6 protein levels decreased in response to Pi through the 26S proteasome degradation machinery using the F-box PRU1 (Ye et al., 2018), which is tightly regulated by Pi starvation but not by As(V) (Castrillo et al., 2013).

In summary, we provide new insights into the molecular mechanisms that underlie the response to As(V), revealing the capacity of As(III) to control PHR1 stability (Figure 7F). The use of As(III) as a signal in As(V) responses provides a selective mode versus Pi to adapt the expression of the Pi transporter in coordination with arsenic detoxification efficiency. The discovery of PHR1 degradation via the proteasome in response to As(III) adds a new regulatory layer in the control of the activity of this master transcription factor.

Although other elements of the As(III) sensing machinery remain unknown in plants, we envision the discovery of a master regulator of the arsenic response, whose activity would be stabilized through direct interaction with As(III), as has been suggested in yeast (Kumar et al., 2015; Di and Tamás, 2007). The identification of key regulatory factors in arsenic signaling will be a major achievement in understanding the mechanisms that underlie arsenic perception in plants and a first step toward the development of new bioremediation and biofortification strategies.

MATERIALS AND METHODS

Plant materials and growth conditions

All *Arabidopsis* lines used in this work were in the Col-0 background. The *cad1-3* mutant (Howden et al., 1995), *phr1-1* mutant (Rubio et al., 2001), Ox*BES1:GFP* (Martínez et al., 2018), 35S::*PHT1;1*:*GFP* (González et al., 2005), and transgenic Ox*PHR1* plants that express PHR1 fused to the HA-tagged hormone ligand domain of the rat glucocorticoid receptor (GR) in the *phr1-1* mutant background (Bustos et al., 2010) were reported previously. A transgenic line expressing 3,847 base pairs (bp) of the *PHR1* genomic region, including 1,787 bp upstream of the ATG, fused to GFP in the *phr1-1* mutant background (*pPHR1::PHR1-GFP*) (Puga et al., 2014) was kindly donated by Dr. V. Rubio and Prof. J. Paz-Ares (Centro Nacional de Biotecnología-CSIC, Madrid). The T-DNA mutants *ask18-1* (GK-014H04), *ask18-2* (SALK-077963.55.50), *phif1-1* (SALK_142735C), and *phif1-2* (SAIL-889-E03) were obtained from the Nottingham *Arabidopsis* Stock Center (NASC). The T-DNA lines were PCR-genotyped to identify plants with homozygous T-DNA insertions (primers listed in Supplemental Table 2).

Seedlings were grown on Johnson medium (Johnson et al., 1957) supplemented with 1% (w/v) sucrose and Pi (KH_2PO_4), As(V) ($NaH_2AsO_4 \cdot 7H_2O$), or As(III) ($NaAsO_2$) at specific concentrations, as indicated for each experiment. Medium was supplemented with 0.6% (w/v) Bacto-Agar (BD Difco) for horizontal plates or 0.9% (w/v) Bacto-Agar (BD Difco) for vertical plates. Plants were grown in a culture chamber with a 16-h light/8-h dark regimen (24°C/21°C).

Arsenic treatments

For the different arsenic treatments, plants were germinated on solid Johnson medium with 1 mM Pi (J+Pi) for 7 days and then transferred to Pi-free Johnson medium (J-Pi), with only traces of Pi from the agar, for 2 days to induce the response to phosphate starvation. These plants were treated with arsenic or Pi in liquid J-Pi medium as indicated in the corresponding experiments. The concentrations used were 30 μM As(V), 60 μM As(III), and 30 μM Pi, unless otherwise stated. For Ox*PHR1* lines, 5 μM dexamethasone (DEX) was included in the J-Pi plates and all subsequent treatments. For proteasome inhibitor treatments, plants were pretreated for 2 h in J-Pi liquid medium with 50 μM MG132 before the addition of 30 μM As(V) or 30 μM Pi for the indicated time periods.

For As(V) tolerance analysis, plants were grown on plates of Johnson medium with the indicated As(V) concentrations, and primary root lengths were measured using ImageJ software (Schindelin et al., 2012). Tolerance was represented as relative root length, calculated as the ratio of primary root length of each individual in control or As(V) supplemented plates to the average primary root length of the corresponding genotype under control conditions. The number of plant roots measured for each experiment is indicated in the manuscript. Differences among genotypes were compared using Student's t test or ANOVA as indicated in the manuscript; p values lower than 0.005 were considered to be statistically significant.

Please cite this article in press as: Navarro et al., Arsenite provides a selective signal that coordinates arsenate uptake and detoxification through the regulation of PHR1 stability in *Arabidopsis*, Molecular Plant (2021), https://doi.org/10.1016/j.molp.2021.05.020

Arsenic quantification

For total arsenic quantification, approximately 100 9-day-old seedlings were treated with 30 μM As(V) as described above, dried, and ground using a mortar. Then, 50 mg of the resulting powder was digested in a microwave oven (Millestone Ethos Easy) with 6 mL of 65% HNO_3 and 2 mL of 33% H_2O_2 at 200°C for 20 min, and the resulting solution was diluted to 20 mL with ultrapure water. Arsenic concentrations in digested seedling solutions were analyzed by ICP-OES iCAP 7400 (Thermo Fisher).

Arsenic species analysis was performed as described previously (Sánchez-Bermejo et al., 2014). Arsenic species from plant samples were extracted with (1:1) methanol:water using a SONOPLUS HD 2200 ultrasonic homogenizer (30%, 60 s). Extracts were centrifuged (5,500 × *g*, 10 min), and the supernatant was filtered before injection into the HPLC. Diluted samples were injected into a PRP-X100 anion-exchange column (250 mm × 4.1 mm, particle size 10 μm; Hamilton, Reno, NV). Arsenic species were eluted in 10 mM $HPO_4^{-2}/H_2PO_4^{-1}$ with a 2% (v/v) MeOH mobile phase at a 1.5 mL min^{-1} flow rate. To test the efficiency of the applied method, the extracts were individually digested with HNO_3-H_2O_2 to compare the total arsenic content determined using inductively coupled plasma mass spectrometry (ICP-MS), with the sum of all arsenic species determined using liquid chromatography (LC)-ICP-MS in the initial extracts. As(III) was quantified using an As(III) calibration curve; As(V) in the sample was used as an internal normalization standard.

Analytical quality control used for total arsenic content and arsenic species was validated by analyzing several Certified Reference Materials (reference numbers SRM 1568a; NIST, USA and CRM-627; BCR, Belgium). Good agreement was found for both reference materials tested (<10% uncertainty based on a 95% confidence level). Extraction recovery was performed by spiking the samples with known amounts of different arsenic species with a recovery efficiency between 80–100%. Arsenic accumulation values were compared using Student's t test, and p values lower than 0.05 were considered to be statistically significant.

Anthocyanin and cellular free phosphate quantification

Anthocyanin was extracted from rosettes of plants grown on J-Pi medium supplemented with 5 μM DEX for 12 days. Anthocyanin content was measured as described previously (Swain and Hillis, 1959). Plant material was extracted at 4°C in the dark for 24 h with solution I (0.5 N HCL, 80% methanol). Subsequently, an equal volume of solution II (3 N HCl, 16.67% methanol) was added. The relative level of anthocyanins was calculated using the absorbance at 530 nm and 637 nm according to the following formula ($A_{530nm} - [-0.25 \times A_{657nm}]$) × dilution factor.

For the cellular free Pi determination, plants were grown on Johnson medium with 1 mM Pi for 7 days, then transferred to Pi-free Johnson medium (J-Pi) for 4 days, and subsequently transferred to plates of J-Pi or to Johnson's plates containing 40 μM Pi. After 24 h, plants were collected, and Pi content was evaluated by the molybdate colorimetric method (Ames, 1966) based on the reduction of the phosphomolybdate complex by ascorbic acid; 1% acetic acid was added to the plant material. After three freeze-thaw cycles to facilitate the release of free Pi, an aliquot of the extract was added to freshly prepared ascorbic acid:molybdate reagent prepared by mixing one volume of 10% ascorbic acid with five volumes of molybdate:H_2SO_4 (0.42% ammonium molybdate, 3.66% H_2SO_4). After incubation at 37°C for 1 h, absorbance at 820 nm was determined, and free Pi was calculated using a standard curve. Free Pi content values were compared using Student's t test, and p values lower than 0.05 were considered to be statistically significant.

Binary construct and plant transformation

To generate Ox*ASK18*/Ox*PHR1* double transgenic lines, the full-length *ASK18* coding sequence was amplified using ASK18_for and ASK18_rev primers (Supplemental Table 2), cloned into the pENTR/D-TOPO vector (Invitrogen), and inserted into the pGWB402 binary vector (Nakagawa et al., 2007b) containing the constitutive CaMV 35S promoter using the LR recombination reaction (Invitrogen). This binary construct was introduced into *Agrobacterium tumefaciens* strain C58C1 and transformed into the previously generated Ox*PHR1 Arabidopsis* transgenic line (Bustos et al., 2010). Transformants were selected on 50 mg/L kanamycin and 10 mg/L BASTA-containing medium.

Subcellular localization analysis

To study the subcellular localization of the ASK18 protein, its full-length coding sequence was amplified as above and cloned into the pGWB6 plasmid (Nakagawa et al., 2007a) to obtain GFP-ASK18 fusion protein under the control of the CaMV 35S promoter. *N. benthamiana* leaves were transiently transformed by agroinfiltration with this construct and with the suppressor of silencing p19 (1:1) as described previously (Voinnet et al., 2003). Subcellular localization was observed in epidermal cells 72 h after agroinfiltration using a TCS SP5 confocal multispectral system with LAS AF v.2.3.6 software (Leica Microsystems).

Five-day-old 35S::*PHT1;1*:*GFP* plants grown in J-Pi were transferred to J-Pi liquid medium containing 30 μM As(V) or 60 μM As(III) or arsenic-free control medium for 3 h. Plants were then washed for 2 h with water to remove As(V) or As(III). Root epidermal cells from plants before and after the wash were observed using a Leica STELLARIS 5 confocal multispectral system with an integrated software module for real-time multidimensional super-resolution image detection and processing. GFP fluorescence was excited with a 488-nm argon laser line.

Gene expression analyses

Total RNA was extracted using a Z6 buffer protocol as described in Logemann et al. (1987). Plant material was homogenized in Z6 buffer (8 M guanidine hydrochloride, 20 mM MES [4-morpholine ethane sulfonic acid], 20 mM EDTA, 50 mM 2-mercaptoethanol, pH 7) followed by extraction with phenol/chloroform/isoamyl alcohol. Total RNA was precipitated from the aqueous phase, washed with 3 M sodium acetate and 70% ethanol, and dissolved in water. 2 μg of total RNA were treated with the TURBO DNA-free kit (Ambion) and used for cDNA synthesis with the High-Capacity cDNA Reverse Transcription Kit (Applied Biosystems) following the manufacturer's instructions. 0.5 μL of the resulting cDNA was used as a template for PCR analysis in a total volume of 15 μL. qRT-PCR was performed using the SYBR Green reagent (Roche) in a 7500 Real Time PCR system (Applied Biosystems). Three independent biological samples consisting of at least 15 seedlings were used for each treatment. Each sample was normalized using the expression of the housekeeping gene *EF1ALPHA* or *ACT8*. Expression values were compared using Student's t test or ANOVA, as indicated in the manuscript. Primers used are listed in Supplemental Table 2.

Yeast two-hybrid interaction assays

Full-length open reading frames (ORFs) encoding the proteins tested for interaction were cloned into both the *pGADT7* and *pGBKT7* vectors (Clontech) to obtain a translational fusion with the GAL4 activation domain (prey) and binding domain (bait), respectively. The list of primers used can be found in Supplemental Table 2. Yeast two-hybrid experiments were performed using the Matchmaker system (Clontech) according to the manufacturer's instructions. Yeast was co-transformed by heat shock with the indicated combination of bait and prey proteins. Double-transformed yeasts were selected on SD minimal medium lacking tryptophan and leucine (SD-WL). Positive interactions were identified by growth on SD minimal medium lacking tryptophan, leucine, histidine, and adenine (SD-WLHA). The corresponding empty vectors were used as negative controls.

Western blot analyses

Western blot analyses were performed using standard procedures. Plants from the *pPHR1::PHR1-GFP,* Ox*PHR1, OxBES1:GFP*, and *35S::PHT1;1:GFP* lines were treated as specified above. Plants were

Please cite this article in press as: Navarro et al., Arsenite provides a selective signal that coordinates arsenate uptake and detoxification through the regulation of PHR1 stability in *Arabidopsis*, Molecular Plant (2021), https://doi.org/10.1016/j.molp.2021.05.020

germinated on solid Johnson medium with 1 mM Pi (J+Pi) for 7 days, transferred to J-Pi medium for 2 days, and subsequently treated with arsenic or Pi in liquid J-Pi medium as indicated in the corresponding experiments. The concentrations used were 30 μM As(V), 90 μM As(III), and 30 μM Pi, unless otherwise stated. For Ox*PHR1* lines, 5 μM DEX was included in J-Pi plates and all subsequent treatments. For proteasome inhibitor treatments, plants were pretreated for 2 h in J-Pi liquid medium with 50 μM MG132 before addition of 30 μM As(V) or 30 μM Pi for the indicated time periods. Root material was collected and frozen. Proteins from p*PHR1*::*PHR1-GFP*, Ox*BES1:GFP*, and Ox*PHR1* roots were extracted with lysis buffer 1 (50 mM Tris-HCl [pH 7.5], 150 mM NaCl, 0.1% Nonidet-P40 [v/v], 1 mM PMSF, and protease inhibitor cocktail [Roche]). For agroinfiltrated *N. benthamiana* leaves, lysis buffer was supplemented with 10 mM 2-mercaptoethanol. For PHT1;1:GFP protein extraction, root material was homogenized in a buffer containing 125 mM Tris-HCl (pH 7.4), 0.2% SDS, 10% glycerol, 6 M urea, and 1% 2-mercaptoethanol. The amount of protein extract separated by SDS-PAGE was 60 μg for pPHR1::PHR1:GFP, 15 μg for OxPHR1 (HA:GR:PHR1), 30 μg for OxBES1:GFP, and 20 μg for 35S::PHT1;1:GFP protein extracts. Antibodies used for western blots, as well as for pull-down, co-immunoprecipitation, and *in vivo* protein degradation assays are as follows: anti-GFP-HRP (Milteny Biotec #130-091-833) 1/1,000, anti-HA-HRP (Milteny Biotec #130-091-972) 1/2,000, monoclonal anti-ACTIN (SIGMA, A0480) 1/2500, and ProteinA-HRP (Merck 18–160) 1/10,000.

Adjusted relative intensity of the immunodetected protein bands was quantified using ImageJ software (Schindelin et al., 2012). Intensities of the bands were expressed relative to the first lane of each gel, unless otherwise stated, and normalized to the signal intensity of the corresponding internal loading control.

Semi *in vivo* MBP pull-down assays

MBP-PHIF1 recombinant fusion protein and MBP protein were expressed in the *Escherichia coli* BL21 strain carrying the corresponding coding sequence cloned into the pKM596 plasmid, a gift from David Waugh (Addgene plasmid # 8837). For protein expression, exponentially growing *E. coli* cultures (OD_{600nm} = 0.5) were induced with 0.1 mM isopropyl-β-D-thiogalactopyranoside at room temperature for 2 h, lysed using an ultrasonic generator homogenizer (LABSONIC U, BRAUN), and centrifuged at 16,000 × *g* for 30 min at 4°C. Recombinant proteins were purified using 400 μL of amylose resin following the manufacturer's instructions (New England BioLabs #E8021S).

Wild-type or Ox*PHR1* plants were treated with 30 μM As(V) for 2 h, and proteins were extracted from roots with lysis buffer 2 (20 mM Tris-HCl [pH 7.5], 75 mM NaCl, 0.1% Nonidet-P40 [v/v], 0.05% sodium deoxycholate [v/v], 10 mM 2-mercaptoethanol, 2 mM PMSF, and protease inhibitor cocktail [Roche]). Control untreated plants were processed in parallel. Equal amounts of protein extracts were combined with MBP-PHIF1 or MBP protein alone, bound to the amylose resin (New England BioLabs) at 4°C with rotation for 3 h, then washed four times with 1 mL of lysis buffer 2 and eluted in denaturing sample buffer before immunoblot analysis with anti-HA-HRP (1/1000) to detect HA-tagged PHR1 and with anti-ACTIN (1/2500) as a loading control. The input MBP-tagged bait proteins and 1/10 of the pulled-down eluate were stained with Coomassie Brilliant Blue. Adjusted relative intensity of the immunodetected protein bands was quantified using ImageJ software (Schindelin et al., 2012). Intensities of the bands were expressed relative to the first input lane and normalized with respect to the corresponding input actin loading control. Intensity of the Coomassie-stained proteins was expressed relative to the corresponding input protein intensity.

Co-immunoprecipitation assays

To analyze the interaction between PHR1 and the F-box protein PHIF1, the corresponding full ORFs were cloned into pGWB415 and pGWB406, respectively, under the control of the CaMV 35S promoter to obtain the tagged proteins HA-PHR1 and PHIF1-GFP. HA-PHR1 was transiently expressed in combination with PHIF1-GFP or GFP alone and with the suppressor of silencing p19 (1:1:1) in *N. benthamiana* leaves (Voinnet et al., 2003). Proteins were extracted with lysis buffer 2 (20 mM Tris-HCl [pH 7.5], 75 mM NaCl, 0.1% Nonidet-P40 [v/v], 0.05% sodium deoxycholate [v/v], 10 mM 2-mercaptoethanol, 2 mM PMSF, and protease inhibitor cocktail [Roche]). Equal amounts of protein extracts were immunoprecipitated using 4 μL of anti-GFP antibody (MBL #598) bound to 50 μL of Dynabeads Protein G (Invitrogen #10003D) per sample. Immunoprecipitated proteins were detected with anti-GFP-HRP antibody (Milteny Biotec #130-091-833) 1/1,000, and co-immunoprecipitated interacting proteins were detected with anti-HA-HRP antibody (Milteny Biotec #130-091-972) 1/1,000.

In vivo protein degradation assays

Full-length coding sequences of *PHR1* and *PHIF1* were cloned into pGWB406 and pGWB614, respectively, under the control of the CaMV 35S promoter to obtain the tagged proteins GFP-PHR1 and PHIF1-HA. GFP1-PHR1 and GFP alone were transiently co-expressed in *N. benthamiana* leaves with different ratios of PHIF1-HA, as indicated in the article. Three days after infiltration, leaf samples were collected for analysis, and proteins were extracted with lysis buffer 1 (50 mM Tris-HCl [pH 7.5], 150 mM NaCl, 0.1% Nonidet-P40 [v/v], 1 mM PMSF, and protease inhibitor cocktail [Roche]) supplemented with 10 mM 2-mercaptoethanol and immunoblotted with anti-HA-HRP antibody (Milteny Biotec #130-091-972) 1/1,000 and anti-GFP-HRP (Milteny Biotec #130-091-833) 1/1,000 antibodies.

ACCESSION NUMBERS

Arabidopsis Genome Initiative locus identifiers for the genes mentioned in this article are: AT5G43350 (*PHT1;1*), AT3G23430 (*PHO1*), AT1G62300 (*WRKY6*), AT4G28610 (*PHR1*), AT2G21045 (*ARQ1/HAC1*), AT1G10230 (*ASK18*), AT3G61590 (*HWS*), AT5G49000 (*PHIF1*), AT5G03545 (*At4*), AT4G33030 (*SQD1*), AT2G02990 (*RNS1*), AT5G44570 (*CAD1*), AT1G1 9350 (*BES1*), AT1G49240 (*ACT8*), AT5G60390 (*EF1ALPHA*).

SUPPLEMENTAL INFORMATION

Supplemental information can be found online at *Molecular Plant Online*.

FUNDING

This work was supported by fellowships from the Spanish Ministry of Science and Innovation (MICINN) to C.N., C.M.-E., E.S.-B., and G.C. and by a fellowship from Severo Ochoa Centres of Excellence Grant Programme to C.N. and from La Caixa/CNB International PhD fellowship to T.C.M. This work was funded by Spanish Ministry of Science and Innovation Grants BIO2014-55741-R, BIO2017-87524-R and BIO2017-89530, by the Commission of Science and Technology Grant CTQ2017-83569-C2-1-R, and by the Comunidad of Madrid and European funding from FSE and FEDER programs Grants S2018/BAA-4393 and AVANSECAL-II-CM.

AUTHOR CONTRIBUTIONS

C.N., C.M.-E., and T.C.M. performed most of the experimental work and therefore all contributed equally to this work. E.S.-B. was involved in the *ASK18* phenotyping, J.P.-A. in PHR1 degradation analysis, and O.U., M.N.F.-M., J.M.G.-M., and R.M. in all arsenic determination and speciation analysis. J.P.-A., G.C., and A.L. analyzed the data, and A.L. and G.C. designed experiments with contributions from J.P.-A., C.N., C.M.-E., and T.C.M. G.C. and A.L. wrote the paper with contributions from all authors.

ACKNOWLEDGMENTS

We thank Carmen L. Torán for critical reading of the manuscript. We also thank Enrique Rojo de la Viesca for his help with the PHT1; 1:GFP protein localization, the Advanced Light Microscopy unit at the CNB (CSIC), and

Yolanda Leo-del Puerto for technical assistance. The authors declare that they have no conflicts of interest.

Received: September 25, 2020
Revised: April 30, 2021
Accepted: May 24, 2021
Published: May 25, 2021

REFERENCES

Ames, B.N. (1966). Assay of inorganic phosphate, total phosphate and phosphatases. Methods Enzymol. **8**:115–118.

Ashraf, M.A., Umetsu, K., Ponomarenko, O., Saito, M., Aslam, M., Antipova, O., Dolgova, N., Kiani, C.D., Nehzati, S., Tanoi, K., et al. (2020). PIN FORMED 2 modulates the transport of arsenite in Arabidopsis thaliana. Plant Commun. **1**:100009.

Ban, Z., and Estelle, M. (2021). CUL3 E3 ligases in plant development and environmental response. Nat. Plants **7**:6–16.

Bayle, V., Arrighi, J.F., Creff, A., Nespoulous, C., Vialaret, J., Rossignol, M., Gonzalez, E., Paz-Ares, J., and Nussaume, L. (2011). Arabidopsis thaliana high-affinity phosphate transporters exhibit multiple levels of posttranslational regulation. Plant Cell **23**:1523–1535.

Bienert, G.P., Thorsen, M., Schüssler, M.D., Nilsson, H.R., Wagner, A., Tamás, M.J., and Jahn, T.P. (2008). A subgroup of plant aquaporins facilitate the bi-directional diffusion of As(OH)3 and Sb(OH)3 across membranes. BMC Biol. **6**:26.

Bleeker, P.M., Schat, H., Vooijs, R., Verkleij, J.A.C., and Ernst, W.H.O. (2003). Mechanisms of arsenate tolerance in Cytisus striatus. New Phytol. **157**:33–38.

Bustos, R., Castrillo, G., Linhares, F., Puga, M.I., Rubio, V., Pérez-Pérez, J., Solano, R., Leyva, A., and Paz-Ares, J. (2010). A central regulatory system largely controls transcriptional activation and repression responses to phosphate starvation in arabidopsis. PLoS Genet. **6**:e1001102.

Cai, C., Lanman, A., Withers, K.A., DeLeon, A.M., Wu, Q., Gribskov, M., Salt, D.E., and Banks, J.O. (2019). Three genes define a bacterial-like arsenic tolerance. Mechanism in the arsenic hyperaccumulating fern pteris vittata. Curr. Biol. **29**:1625–1633.

Castrillo, G., Sánchez-Bermejo, E., de Lorenzo, L., Crevillén, P., Fraile-Escanciano, A., Mohan, T.C., Mouriz, A., Catarecha, P., Sobrino-Plata, J., Olsson, S., et al. (2013). WRKY6 transcription factor restricts arsenate uptake and transposon activation in Arabidopsis. Plant Cell **25**:2944–2957.

Catarecha, P., Segura, M.D., Franco-Zorrilla, J.M., García-Ponce, B., Lanza, M., Solano, R., Paz-Ares, J., and Leyva, A. (2007). A mutant of the Arabidopsis phosphate transporter PHT1;1 displays enhanced arsenic accumulation. Plant Cell **19**:1123–1133.

Chao, D.Y., Chen, Y., Chen, J., Shi, S., Chen, Z., Wang, C., Danku, J.M., Zhao, F.J., and Salt, D.E. (2014). Genome-wide association mapping identifies a new arsenate reductase enzyme critical for limiting arsenic accumulation in plants. PLoS Biol. **12**:e1002009.

Chen, J., Wang, Y., Wang, F., Yang, J., Gao, M., Li, C., Liu, Y., Liu, Y., Yamaji, N., Ma, J.F., et al. (2015). The rice CK2 kinase regulates trafficking of phosphate transporters in response to phosphate levels. Plant Cell **27**:711–723.

Chen, J., Yoshinaga, M., Garbinski, L.D., and Rosen, B.P. (2016). Synergistic interaction of glyceraldehydes-3-phosphate dehydrogenase and ArsJ, a novel organoarsenical efflux permease, confers arsenate resistance. Mol. Microbiol. **100**:945–953.

Chen, L., and Hellmann, H. (2013). Plant E3 ligases: flexible enzymes in a sessile world. Mol. Plant **6**:1388–1404.

Chen, S.C., Sun, G.X., Yan, Y., Konstantinidis, K.T., Zhang, S.Y., Deng, Y., Li, X.M., Cui, H.L., Musat, F., Popp, D., et al. (2020). The Great Oxidation Event expanded the genetic repertoire of arsenic metabolism and cycling. Proc. Natl. Acad. Sci. U S A **117**:10414–10421.

Chen, Y.F., Li, L.Q., Xu, Q., Kong, Y.H., Wang, H., and Wu, W.H. (2009). The WRKY6 transcription factor modulates PHOSPHATE1 expression in response to low pi stress in arabidopsis. Plant Cell **21**:3554–3566.

Cho, S.K., Ryu, M.Y., Kim, J.H., Hong, J.S., Oh, T.R., Kim, W.T., and Yang, S.W. (2017). RING E3 ligases: key regulatory elements are involved in abiotic stress responses in plants. BMB Rep. **50**:393–400.

Dezfulian, M.H., Soulliere, D.M., Dhaliwal, R.K., Sareen, M., and Crosby, W.L. (2012). The SKP1-like gene family of arabidopsis exhibits a high degree of differential gene expression and gene product interaction during development. PLoS One **7**:e50984.

Di, Y., and Tamás, M.J. (2007). Regulation of the arsenic-responsive transcription factor Yap8p involves the ubiquitin-proteasome pathway. J. Cell Sci. **120**:256–264.

Dong, S., Lau, V., Song, R., Ierullo, M., Esteban, E., Wu, Y., Sivieng, T., Nahal, H., Gaudinier, A., Pasha, A., et al. (2019). Proteome-wide, structure-based prediction of protein-protein interactions/new molecular interactions viewer. Plant Physiol. **179**:1893–1907.

Geisler-Lee, J., O'Toole, N., Ammar, R., Provart, N.J., Millar, A.H., and Geisler, M. (2007). A predicted interactome for arabidopsis. Plant Physiol. **145**:317–329.

González, E., Solano, R., Rubio, V., Leyva, A., and Paz-Ares, J. (2005). PHOSPHATE TRANSPORTER TRAFFIC FACILITATOR1 is a plant-specific SEC12-related protein that enables the endoplasmic reticulum exit of a high-affinity phosphate transporter in Arabidopsis. Plant Cell **17**:3500–3512.

Gresser, M.J. (1981). ADP-arsenate. Formation by submitochondrial particles under phosphorylating conditions. J. Biol. Chem. **256**:5981–5983.

Grill, E., Winnacker, E.L., and Zenk, M.H. (1987). Phytochelatins, a class of heavy-metal-binding peptides from plants, are functionally analogous to metallothioneins. Proc. Natl. Acad. Sci. U S A **84**:439–443.

Hamburger, D., Rezzonico, E., Petétot, J.M.D.C., Somerville, C., and Poirier, Y. (2002). Identification and characterization of the Arabidopsis PHO1 gene involved in phosphate loading to the xylem. Plant Cell **14**:889–902.

Himeno, S., Sumi, D., and Fujishiro, H. (2019). Toxicometallomics of cadmium, manganese and arsenic with special reference to the roles of metal transporters. Toxicol. Res. **35**:311–317.

Holford, I.C.R. (1997). Soil phosphorus: its measurement, and its uptake by plants. Aust. J. Soil Res. **35**:227–239.

Howden, R., Goldsbrough, P.B., Andersen, C.R., and Cobbett, C.S. (1995). Cadmium-sensitive, cad1 mutants of Arabidopsis thaliana are phytochelatin deficient. Plant Physiol. **107**:1059–1066.

Hu, B., Jiang, Z., Wang, W., Qiu, Y., Zhang, Z., Liu, Y., Li, A., Gao, X., Liu, L., Qian, Y., et al. (2019). Nitrate–NRT1.1B–SPX4 cascade integrates nitrogen and phosphorus signalling networks in plants. Nat. Plants **5**:401–413.

Hwang, S.G., Park, H.M., Han, A.R., and Jang, C.S. (2016). Molecular characterization of Oryza sativa arsenic-induced RING E3 ligase 1 (OsAIR1): expression patterns, localization, functional interaction, and heterogeneous overexpression. J. Plant Physiol. **191**:140–148.

Hwang, S.G., Chapagain, S., Han, A.R., Park, Y.C., Park, H.M., Kim, Y.H., and Jang, C.S. (2017). Molecular characterization of rice arsenic-induced RING finger E3 ligase 2 (OsAIR2) and its heterogeneous overexpression in Arabidopsis thaliana. Physiol. Plant **161**:372–384.

IARC. (2012). Arsenic, metals, fibres and dusts. IARC Monogr. Eval. Carcinog. Risks Hum. **100C**:11–465.

Indriolo, E., Na, G.N., Ellis, D., Salt, D.E., and Banks, J.A. (2010). A vacuolar arsenite transporter necessary for arsenic tolerance in the arsenic hyperaccumulating fern pteris vittata is missing in flowering plants. Plant Cell **22**:2045–2057.

Johnson, C.M., Stout, P.R., Broyer, T.C., and Carlton, A.B. (1957). Comparative chlorine requirements of different plant species. Plant Soil **8**:337–353.

Kamiya, T., Tanaka, M., Mitani, N., Jian, F.M., Maeshima, M., and Fujiwara, T. (2009). NIP1;1, an aquaporin homolog, determines the arsenite sensitivity of Arabidopsis thaliana. J. Biol. Chem. **284**:2114–2120.

Kamiya, T., Islam, M.R., Duan, G., Uraguchi, S., and Fujiwara, T. (2013). Phosphate deficiency signaling pathway is a target of arsenate and phosphate transporter OsPT1 is involved in as accumulation in shoots of rice. Soil Sci. Plant Nutr. **59**:580–590.

Korshunova, Y.O., Eide, D., Clark, W.G., Guerinot, M. Lou, and Pakrasi, H.B. (1999). The IRT1 protein from Arabidopsis thaliana is a metal transporter with a broad substrate range. Plant Mol. Biol. **40**:37–44.

Kumar, N.V., Yang, J., Pillai, J.K., Rawat, S., Solano, C., Kumar, A., Grøtli, M., Stemmler, T.L., Rosen, B.P., and Tamás, M.J. (2015). Arsenic directly binds to and activates the yeast AP-1-like transcription factor Yap8. Mol. Cell Biol **36**:913–922.

Kurepa, J., Wang, S., Li, Y., and Smalle, J. (2009). Proteasome regulation, plant growth and stress tolerance. Plant Signal. Behav. **4**:924–927.

LeBlanc, M.S., McKinney, E.C., Meagher, R.B., and Smith, A.P. (2013). Hijacking membrane transporters for arsenic phytoextraction. J. Biotechnol. **163**:1–9.

Lee, J.H., and Kim, W.T. (2011). Regulation of abiotic stress signal transduction by E3 ubiquitin ligases in arabidopsis. Mol. Cells **31**:201–208.

Lim, S.D., Hwang, J.G., Han, A.R., Park, Y.C., Lee, C., Ok, Y.S., and Jang, C.S. (2014). Positive regulation of rice RING E3 ligase OsHIR1 in arsenic and cadmium uptakes. Plant Mol. Biol. **85**:365–379.

Liu, W.J., Wood, B.A., Raab, A., McGrath, S.P., Zhao, F.J., and Feldmann, J. (2010). Complexation of arsenite with phytochelatins reduces arsenite efflux and translocation from roots to shoots in Arabidopsis. Plant Physiol. **152**:2211–2221.

Liu, Y., Xie, Y., Wang, H., Ma, X., Yao, W., and Wang, H. (2017). Light and ethylene coordinately regulate the phosphate starvation response through transcriptional regulation of PHOSPHATE STARVATION RESPONSE1. Plant Cell **29**:2269–2284.

Logemann, J., Schell, J., and Willmitzer, L. (1987). Improved method for the isolation of RNA from plant tissues. Anal. Biochem. **163**:16–20.

Long, J.W., and Ray, W.J. (1973). Kinetics and thermodynamics of the formation of glucose arsenate. reaction of glucose arsenate with phosphoglucomutase. Biochemistry **12**:3932–3937.

Lv, Q., Zhong, Y., Wang, Y., Wang, Z., Zhang, L., Shi, J., Wu, Z., Liu, Y., Mao, C., Yi, K., et al. (2014). SPX4 negatively regulates phosphate signaling and homeostasis through its interaction with PHR2 in rice. Plant Cell **26**:1586–1597.

Lyzenga, W.J., and Stone, S.L. (2012). Abiotic stress tolerance mediated by protein ubiquitination. J. Exp. Bot. **63**:599–616.

Ma, F.J., Yamaji, N., Mitani, N., Xu, X.Y., Su, Y.H., McGrath, S.P., and Zhao, F.J. (2008). Transporters of arsenite in rice and their role in arsenic accumulation in rice grain. Proc. Natl. Acad. Sci. U S A **105**:9931–9935.

Martínez, C., Espinosa-Ruíz, A., Lucas, M., Bernardo-García, S., Franco-Zorrilla, J.M., and Prat, S. (2018). PIF 4-induced BR synthesis is critical to diurnal and thermomorphogenic growth. EMBO J. **37**:e99552.

Medici, A., Szponarski, W., Dangeville, P., Safi, A., Dissanayake, I.M., Saenchai, C., Emanuel, A., Rubio, V., Lacombe, B., Ruffel, S., et al. (2019). Identification of molecular integrators shows that nitrogen actively controls the phosphate starvation response in plants. Plant Cell **31**:1171–1184.

Meharg, A.A., and Hartley-Whitaker, J. (2002). Arsenic uptake and metabolism in arsenic resistant and nonresistant plant species. New Phytol. **154**:29–43.

Meharg, A.A., and Macnair, M.R. (1992a). Genetic correlation between arsenate tolerance and the rate of influx of arsenate and phosphate in holcus lanatus L. Heredity (Edinb) **69**:336–341.

Meharg, A.A., and Macnair, M.R. (1992b). Suppression of the high affinity phosphate uptake system: a mechanism of arsenate tolerance in Holcus lanatus L. J. Exp. Bot. **43**:519–524.

Meharg, A.A., and Rahman, M. (2003). Arsenic contamination of Bangladesh paddy field soils: Implications for rice contribution to arsenic consumption. Environ. Sci. Technol. **37**:229–234.

Meharg, A.A., and Macnair, M.R. (1990). An altered phosphate uptake system in arsenate-tolerant Holcus lanatus L. New Phytol. **116**:29–35.

Meharg, A.A., and Macnair, M.R. (1991). The mechanisms of arsenate tolerance in Deschampsia cespitosa (L.) Beauv. and Agrostis capillaris L. Adaptation of the arsenate uptake system. New Phytol. **119**:291–297.

Misson, J., Thibaud, M.C., Bechtold, N., Raghothama, K., and Nussaume, L. (2004). Transcriptional regulation and functional properties of Arabidopsis Pht1;4, a high affinity transporter contributing greatly to phosphate uptake in phosphate deprived plants. Plant Mol. Biol. **55**:727–741.

Miura, K., Rus, A., Sharkhuu, A., Yokoi, S., Karthikeyan, A.S., Raghothama, K.G., Baek, D., Koo, Y.D., Jin, J.B., Bressan, R.A., et al. (2005). The Arabidopsis SUMO E3 ligase SIZ1 controls phosphate deficiency responses. Proc. Natl. Acad. Sci. U S A **102**:7760–7765.

Mukhopadhyay, R., and Rosen, B.P. (2002). Arsenate reductases in prokaryotes and eukaryotes. Environ. Health Perspect. **110** (*Suppl 5*):745–748.

Nakagawa, T., Suzuki, T., Murata, S., Nakamura, S., Hino, T., Maeo, K., Tabata, R., Kawai, T., Tanaka, K., Niwa, Y., et al. (2007a). Improved gateway binary vectors: high-performance vectors for creation of fusion constructs in transgenic analysis of plants. Biosci. Biotechnol. Biochem. **71**:2095–2100.

Nakagawa, T., Kurose, T., Hino, T., Tanaka, K., Kawamukai, M., Niwa, Y., Toyooka, K., Matsuoka, K., Jinbo, T., and Kimura, T. (2007b). Development of series of gateway binary vectors, pGWBs, for realizing efficient construction of fusion genes for plant transformation. J. Biosci. Bioeng. **104**:34–41.

Pan, W., Wu, Y., and Xie, Q. (2019). Regulation of ubiquitination is central to the phosphate starvation response. Trends Plant Sci. **24**:755–769.

Park, J.H., Han, Y.S., Seong, H.J., Ahn, J.S., and Nam, I.H. (2016). Arsenic uptake and speciation in Arabidopsis thaliana under hydroponic conditions. Chemosphere **154**:283–288.

Puga, M.I., Mateos, I., Charukesi, R., Wang, Z., Franco-Zorrilla, J.M., De Lorenzo, L., Irigoyen, M.L., Masiero, S., Bustos, R., Rodríguez, J., et al. (2014). SPX1 is a phosphate-dependent inhibitor of phosphate starvation response 1 in arabidopsis. Proc. Natl. Acad. Sci. U S A **111**:14947–14952.

Puga, M.I., Rojas-Triana, M., de Lorenzo, L., Leyva, A., Rubio, V., and Paz-Ares, J. (2017). Novel signals in the regulation of Pi starvation

responses in plants: facts and promises. Curr. Opin. Plant Biol. **39**:40–49.

Ren, F., Guo, Q.Q., Chang, L.L., Chen, L., Zhao, C.Z., Zhong, H., and Li, X.B. (2012). Brassica napus PHR1 gene encoding a MYB-like protein functions in response to phosphate starvation. PLoS One **7**:e44005.

Ruan, W., Guo, M., Wang, X., Guo, Z., Xu, Z., Xu, L., Zhao, H., Sun, H., Yan, C., and Yi, K. (2019). Two RING-finger ubiquitin E3 ligases regulate the degradation of SPX4, an internal phosphate sensor, for phosphate homeostasis and signaling in rice. Mol. Plant **12**:1060–1074.

Rubio, V., Linhares, F., Solano, R., Martín, A.C., Iglesias, J., Leyva, A., and Paz-Ares, J. (2001). A conserved MYB transcription factor involved in phosphate starvation signaling both in vascular plants and in unicellular algae. Genes Dev. **15**:2122–2133.

Sánchez-Bermejo, E., Castrillo, G., Del Llano, B., Navarro, C., Zarco-Fernández, S., Martinez-Herrera, D.J., Leo-Del Puerto, Y., Muñoz, R., Cámara, C., Paz-Ares, J., et al. (2014). Natural variation in arsenate tolerance identifies an arsenate reductase in Arabidopsis thaliana. Nat. Commun. **5**:4617.

Schindelin, J., Arganda-Carreras, I., Frise, E., Kaynig, V., Longair, M., Pietzsch, T., Preibisch, S., Rueden, C., Saalfeld, S., Schmid, B., et al. (2012). Fiji: an open-source platform for biological-image analysis. Nat. Methods **9**:676–682.

Schmöger, M.E.V., Oven, M., and Grill, E. (2000). Detoxification of arsenic by phytochelatins in plants. Plant Physiol. **122**:793–801.

Shin, H., Shin, H.S., Dewbre, G.R., and Harrison, M.J. (2004). Phosphate transport in Arabidopsis: Pht1;1 and Pht1;4 play a major role in phosphate acquisition from both low- and high-phosphate environments. Plant J. **39**:629–642.

Sneller, F.E.C., Van Heerwaarden, L.M., Kraaijeveld-Smit, F.J.L., Ten Bookum, W.M., Koevoets, P.L.M., Schat, H., and Verkleij, J.A.C. (1999). Toxicity of arsenate in Silene vulgaris, accumulation and degradation of arsenate-induced phytochelatins. New Phytol. **144**:223–232.

Song, W.Y., Park, J., Mendoza-Cózatl, D.G., Suter-Grotemeyer, M., Shima, D., Hörtensteiner, S., Geisler, M., Weder, B., Rea, P.A., Rentsch, D., et al. (2010). Arsenic tolerance in Arabidopsis is mediated by two ABCC-type phytochelatin transporters. Proc. Natl. Acad. Sci. U S A **107**:21187–21192.

Sors, T.G., Ellis, D.R., Gun, N.N., Lahner, B., Lee, S., Leustek, T., Pickering, I.J., and Salt, D.E. (2005). Analysis of sulfur and selenium assimilation in Astragalus plants with varying capacities to accumulate selenium. Plant J. **42**:785–797.

Stone, S.L. (2014). The role of ubiquitin and the 26S proteasome in plant abiotic stress signaling. Front. Plant Sci. **5**:135.

Sung, D.Y., Kim, T.H., Komives, E.A., Mendoza-Cózatl, D.G., and Schroeder, J.I. (2009). ARS5 is a component of the 26S proteasome complex, and negatively regulates thiol biosynthesis and arsenic tolerance in Arabidopsis. Plant J. **59**:802–813.

Swain, T., and Hillis, W.E. (1959). The phenolic constituents of Prunus domestica. I.—the quantitative analysis of phenolic constituents. J. Sci. Food Agric. **10**:63–68.

Thomine, S., Wang, R., Ward, J.M., Crawford, N.M., and Schroeder, J.I. (2000). Cadmium and iron transport by members of a plant metal transporter family in Arabidopsis with homology to Nramp genes. Proc. Natl. Acad. Sci. U S A **97**:4991–4996.

Tripathi, R.D., Srivastava, S., Mishra, S., Singh, N., Tuli, R., Gupta, D.K., and Maathuis, F.J.M. (2007). Arsenic hazards: strategies for tolerance and remediation by plants. Trends Biotechnol. **25**:158–165.

Verbruggen, N., Hermans, C., and Schat, H. (2009). Molecular mechanisms of metal hyperaccumulation in plants. New Phytol. **181**:759–776.

Voinnet, O., Rivas, S., Mestre, P., and Baulcombe, D. (2003). An enhanced transient expression system in plants based on suppression of gene silencing by the p19 protein of tomato bushy stunt virus. Plant J. **33**:949–956.

Wang, J., Sun, J., Miao, J., Guo, J., Shi, Z., He, M., Chen, Y., Zhao, X., Li, B., Han, F.P., et al. (2013a). A phosphate starvation response regulator Ta-PHR1 is involved in phosphate signalling and increases grain yield in wheat. Ann. Bot. **111**:1139–1153.

Wang, X., Bai, J., Liu, H., Sun, Y., Shi, X., and Ren, Z. (2013b). Overexpression of a maize transcription factor ZmPHR1 Improves shoot inorganic phosphate content and growth of arabidopsis under low-phosphate conditions. Plant Mol. Biol. Rep. **31**:665–677.

Wang, Y., Zhang, F., Cui, W., Chen, K., Zhao, R., and Zhang, Z. (2019). The FvPHR1 transcription factor control phosphate homeostasis by transcriptionally regulating miR399a in woodland strawberry. Plant Sci. **280**:258–268.

Williams, P.N., Islam, M.R., Adomako, E.E., Raab, A., Hossain, S.A., Zhu, Y.G., Feldmann, J., and Meharg, A.A. (2006). Increase in rice grain arsenic for regions of Bangladesh irrigating paddies with elevated arsenic in groundwaters. Environ. Sci. Technol. **40**:4903–4908.

Wu, Z., Ren, H., Mcgrath, S.P., Wu, P., and Zhao, F.J. (2011). Investigating the contribution of the phosphate transport pathway to arsenic accumulation in rice. Plant Physiol. **157**:498–508.

Xu, F.Q., and Xue, H.W. (2019). The ubiquitin-proteasome system in plant responses to environments. Plant Cell Environ. **42**:2931–2944.

Xu, W., Dai, W., Yan, H., Li, S., Shen, H., Chen, Y., Xu, H., Sun, Y., He, Z., and Ma, M. (2015). Arabidopsis NIP3;1 plays an important role in arsenic uptake and root-to-shoot translocation under arsenite stress conditions. Mol. Plant **8**:722–733.

Xue, Y. Bin, Xiao, B.X., Zhu, S.N., Mo, X.H., Liang, C.Y., Tian, J., and Liao, H. (2017). GmPHR25, a GmPHR member up-regulated by phosphate starvation, controls phosphate homeostasis in soybean. J. Exp. Bot. **68**:4951–4967.

Yang, J., Xie, M.Y., Wang, L., Yang, Z.L., Tian, Z.H., Wang, Z.Y., Xu, J.M., Liu, B.H., Deng, L.W., Mao, C.Z., et al. (2018). A phosphate-starvation induced RING-type E3 ligase maintains phosphate homeostasis partially through OsSPX2 in rice. Plant Cell Physiol. **59**:2564–2575.

Ye, Q., Wang, H., Su, T., Wu, W.H., and Chen, Y.F. (2018). The ubiquitin E3 ligase PRU1 regulates WRKY6 degradation to modulate phosphate homeostasis in response to low-Pi stress in arabidopsis. Plant Cell **30**:1062–1076.

Zhao, D., Ni, W., Feng, B., Han, T., Petrasek, M.G., and Ma, H. (2003). Members of the Arabidopsis-SKP1-like gene family exhibit a variety of expression patterns and may play diverse roles in arabidopsis. Plant Physiol. **133**:203–217.

Zhao, F.J., Ago, Y., Mitani, N., Li, R.Y., Su, Y.H., Yamaji, N., McGrath, S.P., and Ma, J.F. (2010a). The role of the rice aquaporin Lsi1 in arsenite efflux from roots. New Phytol. **186**:392–399.

Zhao, F.J., Ma, J.F., Meharg, A.A., and McGrath, S.P. (2009). Arsenic uptake and metabolism in plants. New Phytol. **181**:777–794.

Zhao, F.J., McGrath, S.P., and Meharg, A.A. (2010b). Arsenic as a food chain contaminant: mechanisms of plant uptake and metabolism and mitigation strategies. Annu. Rev. Plant Biol. **61**:535–559.

Zhao, X.Q., Mitani, N., Yamaji, N., Shen, R.F., and Ma, J.F. (2010c). Involvement of silicon influx transporter OsNIP2;1 in selenite uptake in rice. Plant Physiol. **153**:1871–1877.

Zheng, N., Schulman, B.A., Song, L., Miller, J.J., Jeffrey, P.D., Wang, P., Chu, C., Koepp, D.M., Elledge, S.J., Pagano, M., et al. (2002). Structure of the Cul1-Rbx1-Skp1-F boxSkp2 SCF ubiquitin ligase complex. Nature **416**:703–709.

Zhou, J., Jiao, F.C., Wu, Z., Li, Y., Wang, X., He, X., Zhong, W., and Wu, P. (2008). OsPHR2 is involved in phosphate-starvation signaling and excessive phosphate accumulation in shoots of plants. Plant Physiol. **146**:1673–1686.

Zhu, Y.G., Sun, G.X., Lei, M., Teng, M., Liu, Y.X., Chen, N.C., Wang, L.H., Carey, A.M., Deacon, C., Raab, A., et al. (2008). High percentage inorganic arsenic content of mining impacted and nonimpacted Chinese rice. Environ. Sci. Technol. **42**:5008–5013.

Zhu, Y.G., Yoshinaga, M., Zhao, F.J., and Rosen, B.P. (2014). Earth abides arsenic biotransformations. Annu. Rev. Earth Planet. Sci. **42**:443–467.

Zvobgo, G., LwalabaWaLwalaba, J., Sagonda, T., Mutemachani Mapodzeke, J., Muhammad, N., Haider Shamsi, I., and Zhang, G. (2018). Phosphate alleviates arsenate toxicity by altering expression of phosphate transporters in the tolerant barley genotypes. Ecotoxicol. Environ. Saf. **147**:832–839.

Molecular Plant, Volume *14*

Supplemental information

Arsenite provides a selective signal that coordinates arsenate uptake and detoxification through the regulation of PHR1 stability in *Arabidopsis*

Cristina Navarro, Cristian Mateo-Elizalde, Thotegowdanapalya C. Mohan, Eduardo Sánchez-Bermejo, Oscar Urrutia, María Nieves Fernández-Muñiz, José M. García-Mina, Riansares Muñoz, Javier Paz-Ares, Gabriel Castrillo, and Antonio Leyva

Supplemental information

ARSENITE PROVIDES A SELECTIVE SIGNAL THAT COORDINATES ARSENATE UPTAKE AND DETOXIFICACION INVOLVING REGULATION OF PHR1 STABILITY IN *ARABIDOPSIS THALIANA*

Cristina Navarro[1,7], Cristian Mateo-Elizalde[1,7], Thotegowdanapalya C. Mohan[1,4,7], Eduardo Sánchez-Bermejo[1,5], Oscar Urrutia[2], María Nieves Fernández-Muñiz[3], José M. García-Mina[2], Riansares Muñoz[3], Javier Paz-Ares[1], Gabriel Castrillo[1,6,*] and Antonio Leyva[1,*]

Affiliations

[1]Department of Plant Molecular Genetics, Centro Nacional de Biotecnología-Consejo Superior de Investigaciones Científicas, 28049, Madrid, Spain

[2]Department of Environmental Biology, Sciences School, University of Navarra, 31008, Pamplona, Spain

[3]Department of Analytical Chemistry, School of Chemical Sciences, Universidad Complutense de Madrid, 28040, Madrid, Spain

***Correspondence:** Gabriel Castrillo (gabriel.castrillo@nottingham.ac.uk), Antonio Leyva (aleyva@cnb.csic.es)

Additional Footnotes

[4]Present address: Department of Biotechnology and Bioinformatics

Faculty of Life Sciences, JSS Academy of Higher Education and Research, Mysuru, 570015, Karnataka, India

[5]Present address: S&A Fresh Produce. Brook Farm, Marden, Hereford HR1 3ET, UK

[6]Present address: Future Food Beacon of Excellence & School of Biosciences, University of Nottingham, Nottingham LE12 5RD, UK

[7]These authors contributed equally to this work

SUPPLEMENTAL INFORMATION

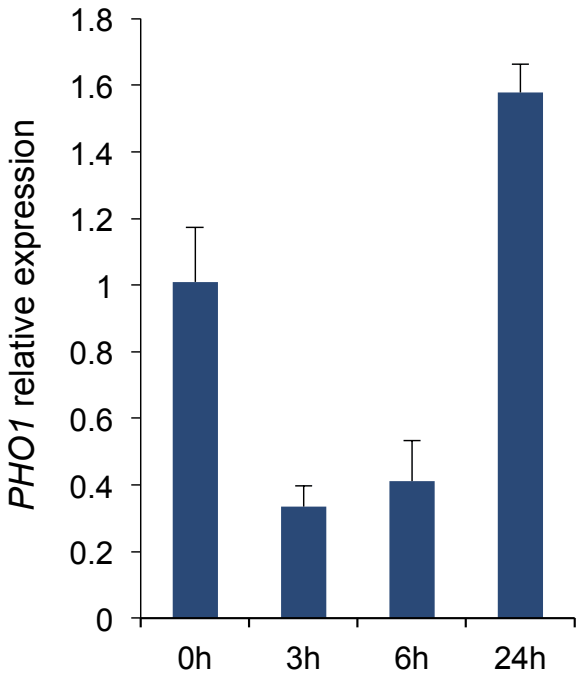

Supplemental Figure 1. qRT-PCR analysis of *PHO1* phosphate transporter kinetics expression in response to As(V). Wild-type plants were grown in solid Johnson medium supplemented with 1 mM Pi in horizontal position for 7 days, transferred to Pi-free conditions for 2 days, and then exposed to 30 µM As(V) in liquid conditions. Gene expression was analyzed in whole plants collected for the analysis at 0, 3, 6, and 24 h post-treatment. Error bars indicate SD. Three independent biological replicates were used, each containing at least 15 plants.

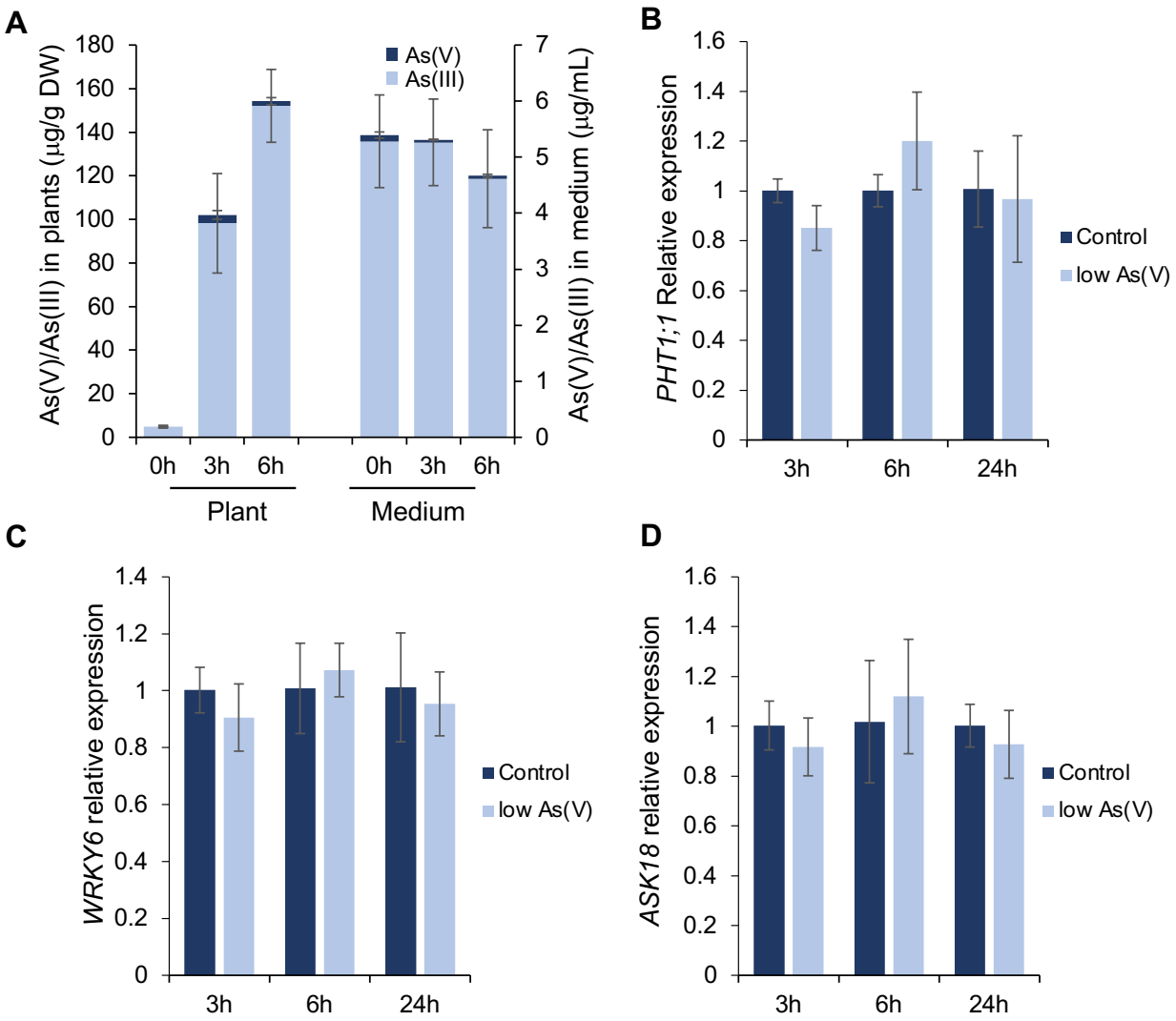

Supplemental Figure 2. *PHT1;1*, and *WRKY6* and *ASK18* transcriptional regulation by As(III) is controlled by this chemical species and not by As(V) derived from As(III) spontaneous oxidation. **(A)** Quantification of arsenic chemical species, As(V) and As(III), in medium and whole plants exposed to 60 µM As(III). Wild-type plants were grown on solid Johnson medium supplemented with 1 mM Pi in horizontal position for 7 days, transferred to Pi-free medium for 2 days, and subsequently treated with 60 µM As(III), in Pi-free liquid medium. Samples (whole plants and medium) were collected at 0, 3, 6 h post-treatment. The data was normalized by the sample dry weight in the case of the plant tissue and by the volume in the case of the medium. Three independent biological replicates were used, each containing at least 45 plants. **(B-D)** qRT-PCR analysis of *PHT1;1* **(B)**, *WRKY6* **(C),** and *ASK18* **(D)** expression in wild-type plants treated or not (control) with 550 nM As(V) (low As(V)), and in the corresponding untreated plants. Plants were grown and treated as described in (A), and exposed to 550 nM As(V). This As(V) concentration was the maximum amount of As(V) detected in the As(III) solution from (A). In all qRT-PCR experiments, three independent biological replicates were used, each containing at least 15 plants. In the figure, error bars indicate SD.

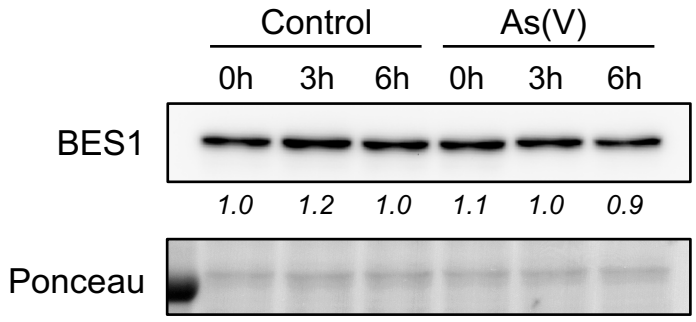

Supplemental Figure 3. BES1 protein is not degraded in response to As(V) treatment. Western blot analysis of BES1, a non-related transcription factor, stability in plants exposed to 30 µM As(V). *BES1-GFP*-overexpressing plants were grown on solid Johnson medium supplemented with 1 mM Pi in horizontal position for 7 days, transferred to Pi-free medium for 2 days, and subsequently treated with 30 µM Pi (control) or 30 µM As(V), in Pi-free liquid medium. For the analysis, root samples were collected at 0, 3, and 6 h post-treatments. Ponceau S staining is used as a loading control. The numbers in italics below the lanes represent the adjusted relative intensity, relativized to the first lane of the gel and normalized with respect to the corresponding loading control.

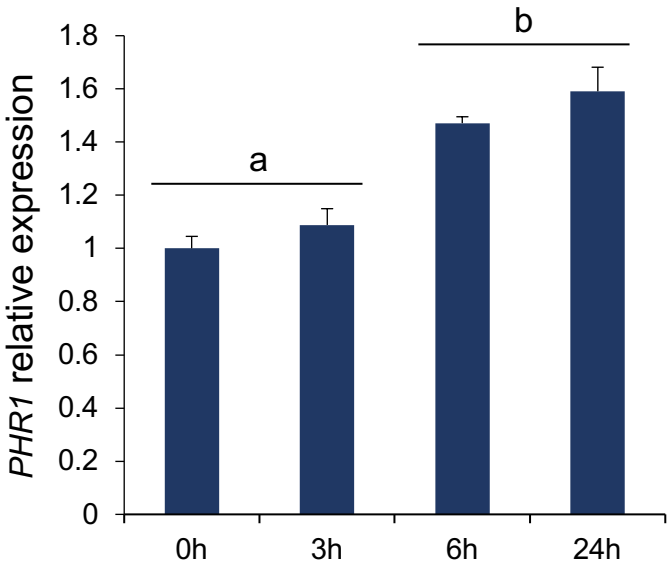

Supplemental Figure 4. qRT-PCR analysis of *PHR1* kinetics expression in response to As(V). Wild-type plants were grown on solid Johnson medium supplemented with 1 mM Pi in horizontal position for 7 days, transferred to low Pi conditions for 2 days, and then exposed to 30 µM As(V) in liquid conditions. Whole plants were collected for the analysis at 0, 3, 6, and 24 h post-treatment. Error bars indicate SD. Three independent biological replicates were used, each consisting of 15 plants. Treatments with the same letter are not significantly different from each other (ANOVA, $p < 0.001$).

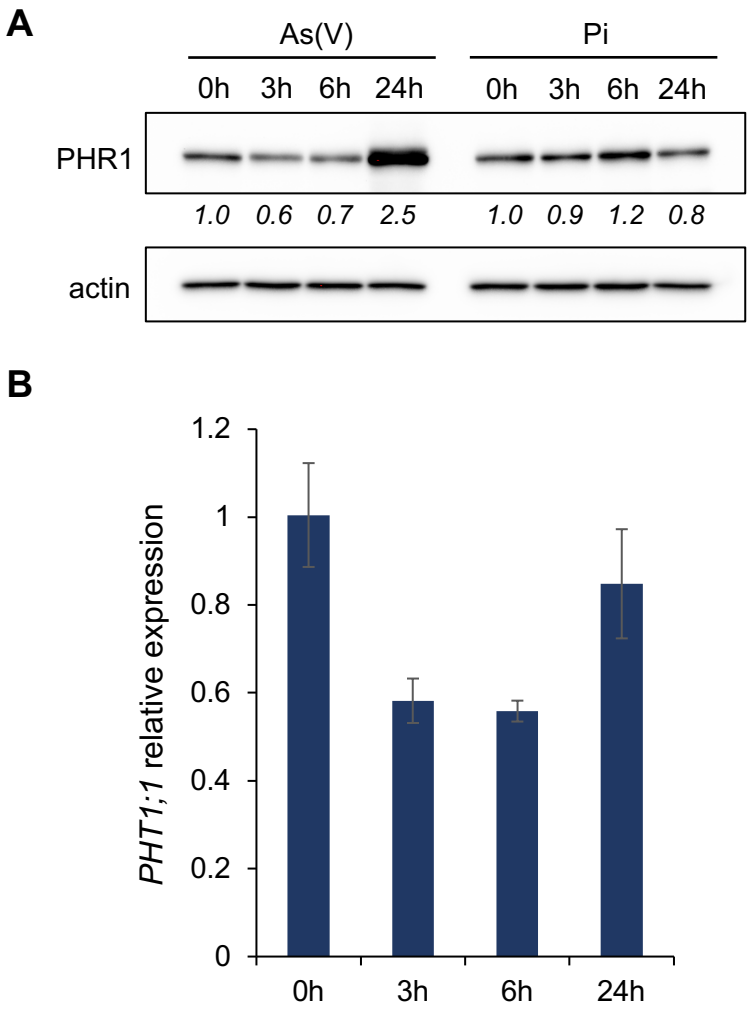

Supplemental Figure 5. *PHT1;1* expression and PHR1 protein levels in PHR1-overexpressing plants (Ox*PHR1*) in response to As(V). (A) Immunoblot analysis of PHR1 protein levels in roots of Ox*PHR1* plants exposed to 30 µM As(V) or 30 µM Pi. Ox*PHR1* plants were grown on solid Johnson medium supplemented with 1 mM Pi in horizontal position for 7 days, transferred to Pi-free medium for 2 days, and then exposed to 30 µM As(V) or 30 µM Pi, in Pi-free liquid medium. Roots were harvested for the analysis at 0, 3, 6, 24h post-treatment. Hybridization with anti-actin antibody is shown as a loading control. The numbers in italics below the lanes represent the adjusted relative intensity, relativized to the first lane of the gel and normalized with respect to the corresponding loading control. **(B)** qRT-PCR analysis of *PHT1;1* kinetic expression in Ox*PHR1* plants exposed to As(V). Ox*PHR1* plants were grown as in (A), and subsequently treated with 30 µM As(V), in Pi-free liquid medium, Whole plants were harvested for the analysis at 0, 3, 6, and 24 h post-treatments. Three independent biological replicates were used, each with 15 plants.

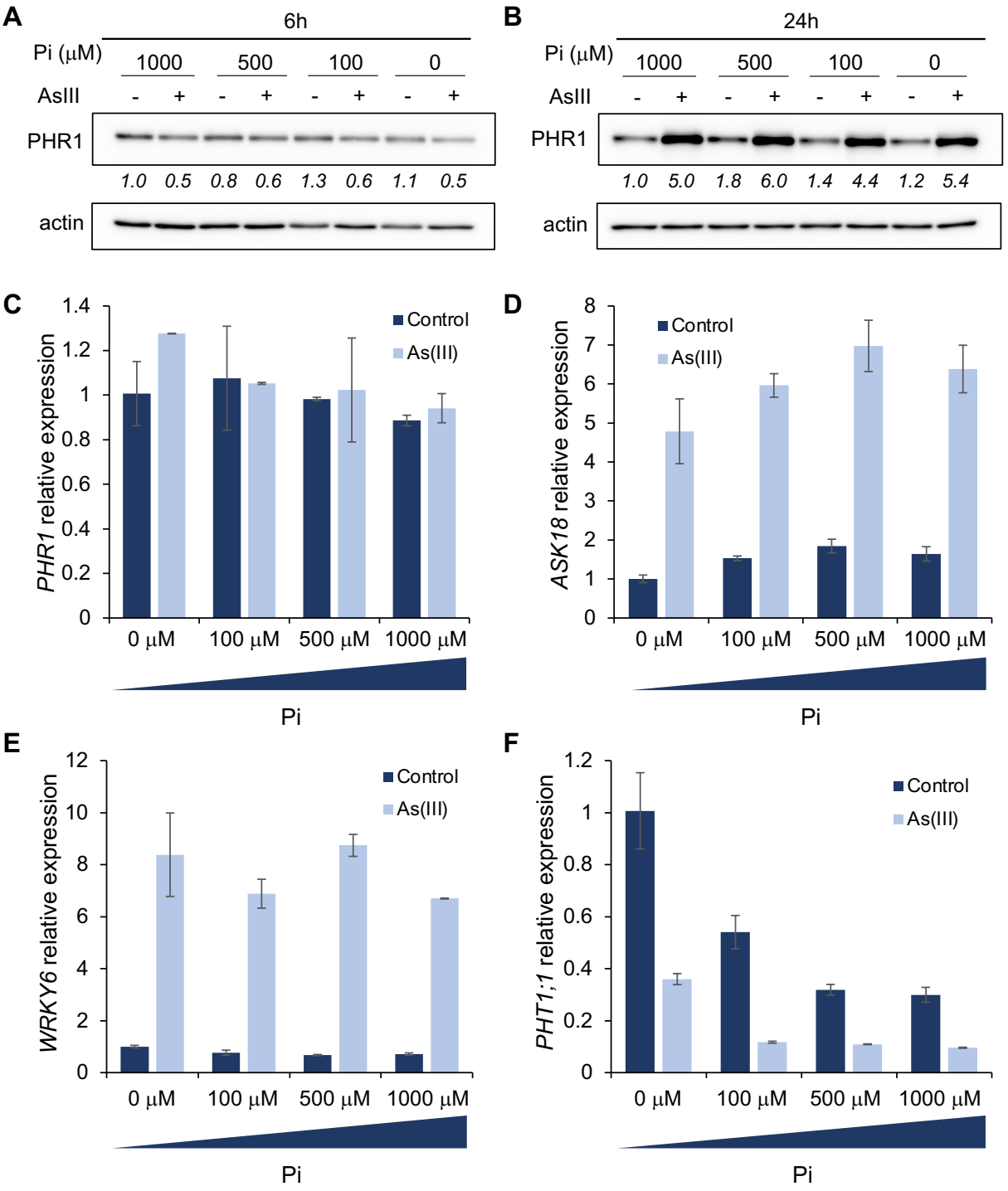

Supplemental Figure 6. Effect of high level of Pi on As(III) response. (A, B) Immunoblot analysis of PHR1 levels in roots of *PHR1*-overexpressing (Ox*PHR1*) plants exposed to 90 µM As(III) in the presence of a gradient of Pi concentrations. Ox*PHR1* plants were grown on solid Johnson medium supplemented with 1 mM Pi in horizontal position for 7 days, transferred to low Pi conditions for 2 days, and then treated (+) or not (-) with 90 µM As(III), in the presence of 0, 100, 500 and 1000 µM Pi, in liquid medium, for 6h **(A)** or 24h **(B).** Hybridization with anti-actin antibody is shown as a loading control. The numbers in italics below the lanes represent the adjusted relative intensity, relativized to the first lane of each gel and normalized with respect to the corresponding loading control. **(C-F)** qRT-PCR analysis of *PHR1* **(C)**, *ASK18* **(D)**, *WRKY6* **(E)**, and *PHT1;1* **(F)** expression in wild-type plants exposed to 60 µM As(III) in the presence of a gradient of Pi concentrations. Wild-type plants were grown on J+Pi (1 mM) horizontal plates for 7 days, transferred to J-Pi horizontal plates without Pi (-Pi), or 100, 500 and 1000 µM Pi for 2 days, and subsequently treated or not (control) with 60 µM As(III), in combination with the indicated concentrations of Pi, in J-Pi liquid medium, for 6 h. Three independent biological replicates, each consisting of 15 plants, were used.

A

	1.5h	8h	
AT1G05890		2.57	RING/U-box superfamily protein
AT1G10230	3.80	7.17	**E3 ubiquitin ligase SCF complex subunit SKP1/ASK1 family**
AT1G17280		2.17	ubiquitin-conjugating enzyme 34
AT1G35625	4.76		RING/U-box superfamily protein
AT1G53750		2.08	26S proteasome AAA-ATPase subunit RPT1a (RPT1a)
AT1G77000		8.42	RNI-like superfamily protein
AT2G22010		2.04	Predicted to act as a RING E3 ubiquitin ligase
AT3G08690		3.43	ubiquitin-conjugating enzyme 11
AT3G20060		2.30	ubiquitin-conjugating enzyme belonging to the E2-C gene family
AT4G03510		3.90	RING membrane-anchor 1
AT4G23570		2.29	SGT1A, may function in SCF(TIR1) mediated protein degradation
AT4G27960	2.32		ubiquitin conjugating enzyme
AT4G34470	5.23		SKP1-like 12
AT5G03240		2.48	UBQ3, ubiquitin attached to proteins destined for degradation
AT5G20910		7.88	Encodes an E3 ligase that can polyubiquitinate ABI3 in vitro
AT5G43190		3.41	Galactose oxidase/kelch repeat superfamily protein
AT5G58290		2.53	26S proteasome AAA-ATPase subunit RPT3 (RPT3)
AT5G62540		7.90	UBC3, predicted to be an E2 ubiquitin conjugating enzyme

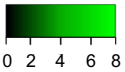

B

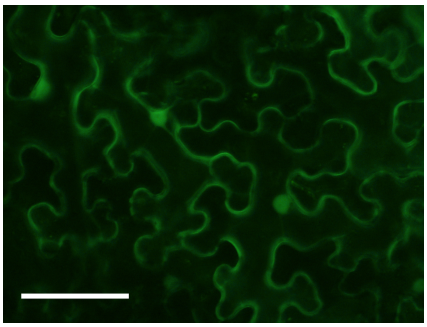

Supplemental Figure 7. Identification of ASK18 (AT1G10230), from a set of ubiquitin-related genes induced by As(V), as a regulatory candidate of PHR1 stability. (A) Heatmap showing the transcriptional activation for the set of genes induced in response to 1.5 and 8 h As(V) treatments (Castrillo et al., 2013) and included in the GO term “ubiquitin-dependent protein catabolic process” (GO:0006511). For each gene, the log2 fold change values of relative As(V) induction are shown. The ASK18 gene (AT1G10230) is highlighted in bold. **(B)** Subcellular localization of GFP-ASK18 in *N. benthamiana* leaves. Scale bar represents 50 μM.

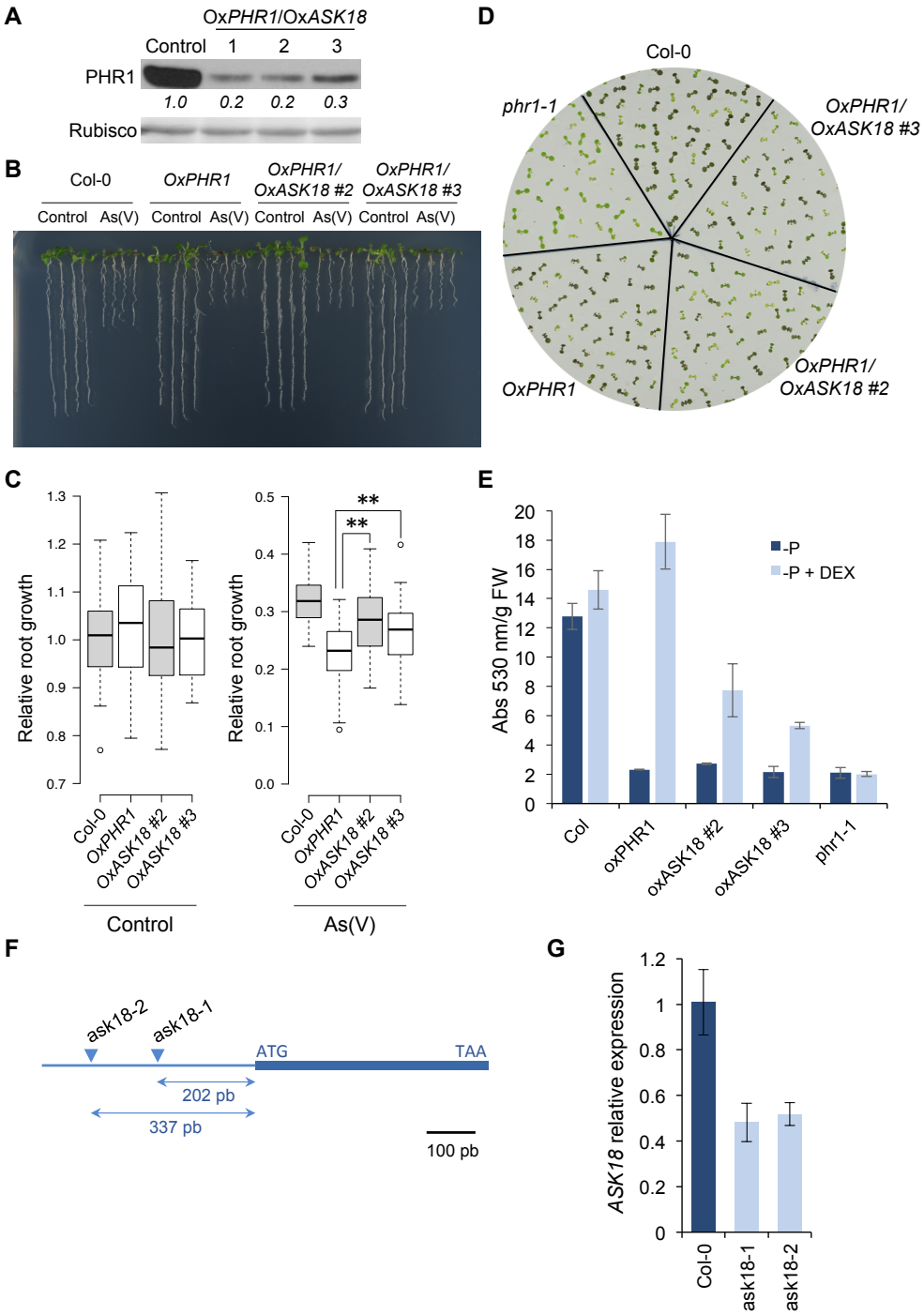

Supplemental Figure 8. ASK18 is a regulator of PHR1 stability. (A) Immunoblot analyses of PHR1-HA protein levels in three lines double overexpressing *ASK18* and *HA*:*GR*:*PHR1* (Ox*PHR1*) in the *phr1-1* mutant background (Ox*PHR1*/Ox*ASK18*). Plants were grown in Johnson medium supplemented with 1 mM Pi for 7 days and then transferred to Pi-free medium with 5 µM dexamethasone (DEX) for 3 days. The levels of HA-PHR1 in root protein extracts from the three lines were analyzed by western blot. The numbers in italics below the lanes represent the adjusted relative band intensity, relativized to the first lane of each gel and normalized with respect to the corresponding loading control. **(B, C)** Phenotypic analysis of two independent lines overexpressing *ASK18* in the Ox*PHR1* background (Ox*PHR1*/Ox*ASK18* lines (#2 and #3)), in response to As(V) treatment. **(B)** As(V) tolerance phenotype of wild-type plants, *HA*:*GR*:*PHR1*-overexpressing (Ox*PHR1*) line in the *phr1-1* mutant background and Ox*PHR1*/Ox*ASK18* #2 and #3 lines grown in vertical plates containing 30 µM Pi alone (control) or in combination with 25 µM As(V), for 8 days. **(C)** Quantification of relative root growth (ratio of primary root length of each individual in control or As(V) supplemented plates, relative to the average of the primary root length of the corresponding genotype in control conditions) of wild-type, Ox*PHR1* and Ox*PHR1*/Ox*ASK18* #2 and #3 lines from the experiment shown in (B). At least 29 plants per genotype were quantified. Asterisks indicate significant differences with the Ox*PHR1* plants (Student's *t*-test, $p < 0.001$). **(D, E)** Anthocyanin accumulation in plants with different levels of PHR1 activity. **(D)** Wild type plants, *PHR1*-overexpressing (Ox*PHR1*) line, two independent lines overexpressing both *PHR1* and *ASK18* (Ox*PHR1*/Ox*ASK18* lines (#2 and #3)), and *phr1* mutant were grown in phosphate-free medium plates supplemented with 5 µM DEX for 12 days. **(E)** The graph shows anthocyanin quantification of plants from the experiment shown in (D). The anthocyanin content, expressed as absorbance at 530 nm, was normalized by the fresh weight (FW) in each case (Abs 530 nm/g FW). For this experiment, three independent biological replicas, each with 15 plants were used. **(F)** Schematic diagram depicting T-DNA insertion positions in the *ask18* mutants identified. The distance from the ATG to the T-DNA border is shown in each case **(G)** qRT-PCR analysis of *ASK18* expression in *ask18-1* and *ask18-2* mutant plants. Plants were grown on solid Johnson medium supplemented with 1 mM Pi for 7 days, and then transferred to Pi-free medium for 2 days. Three independent biological replicas, each consisting of 15 plants, were used. Error bars indicate SD.

A

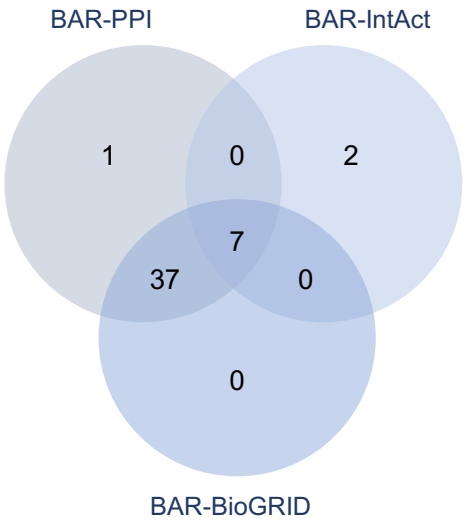

B

AT3G61590	HWS Galactose oxidase/kelch repeat superfamily protein
AT3G63060	EDL3 EID1-like 3 F-box protein involved in the regulation of abscisic acid signalling
AT4G02570	ATCUL1_AXR6_CUL1_ICU13__cullin 1
AT5G49000	**Galactose oxidase/kelch repeat superfamily protein**
AT1G31350	KUF1 KAR-UP F-box 1
AT2G25490	EBF1_FBL6__EIN3-binding F box protein 1
AT5G49610	F-box family protein

Supplemental Figure 9. Identification of F-box proteins interacting with ASK18. (A) Venn analysis of ASK18 interacting proteins, according to the BioGRID, IntAct and PPI-BAR databases from the Bio-Analytic Resource (BAR) interactions viewer 2.0. **(B)** List of the 7 proteins common to the 3 databases analyzed. The list includes the CULLIN1 (AT4G02570) protein and 6 F-boxes. The three F-box proteins (AT5G49610, AT5G49000 and AT3G61590) found interacting with ASK18 in a yeast-two-hybrid assay (Figure 6A) are highlighted with a darker blue fill. Out of these three proteins, the only one (AT5G49000, PHIF1) found interacting with PHR1 in a yeast-two-hybrid assay (Figure 6B) is highlighted in bold.

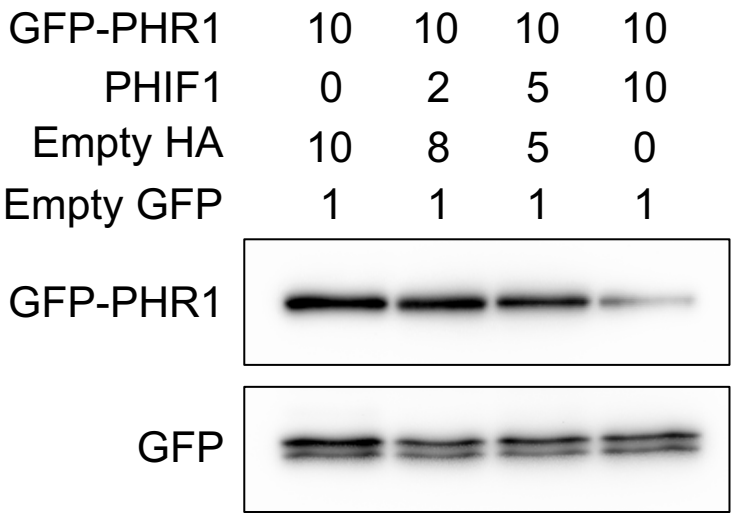

Supplemental Figure 10. *In vivo* degradation assay of PHR1 by PHIF1. GFP-PHR1 and GFP-alone were transiently co-expressed with increasing amounts of non-tagged PHIF1 in *N. benthamiana* leaves. Relative amounts of each construct are indicated by numbers above the blots. Protein extracts were immunoblotted against anti-GFP antibody. GFP alone was used as a control.

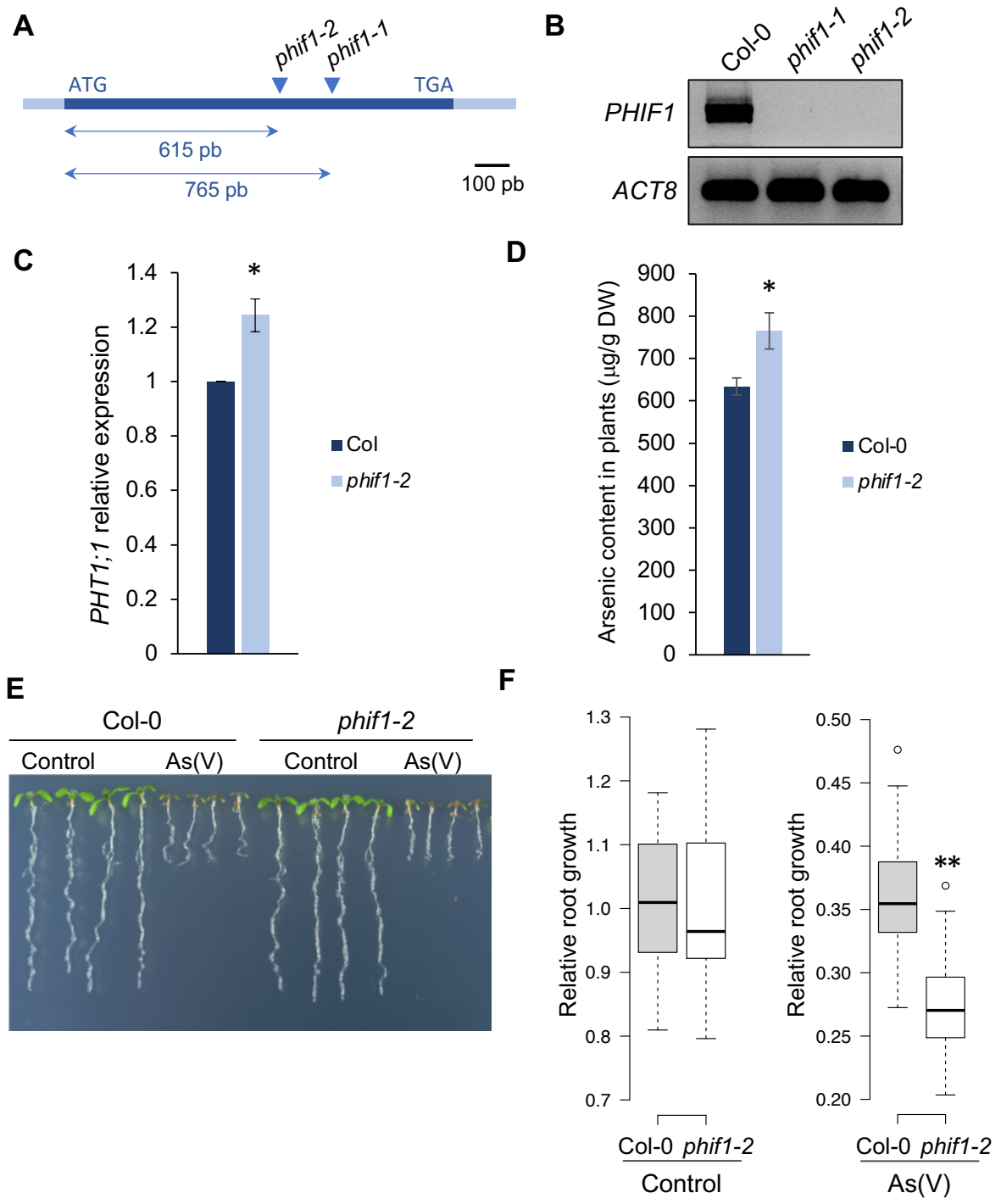

Supplemental Figure 11. F-box protein PHIF1 mediates PHR1 degradation in response to arsenic. (A) Schematic diagram depicting T-DNA insertion positions in the *phif1* mutants (*phif1-1* and *phif1-2*) identified in this work. The distance from the ATG to the T-DNA border is shown in each case. **(B)** RT-PCR analysis of *PHIF1* expression in the *phif1-1* and *phif1-2* mutants. Expression of the *ACTIN8* gene is shown as a control. **(C)** qRT-PCR analysis of *PHT1;1* expression in wild-type plants (Col-0) and *phif1-2* mutants. Plants were grown in solid Johnson medium supplemented with 1mM Pi in horizontal position for 7 days and transferred to Pi-free horizontal plates for 2 days. Three independent biological replicas, each consisting of 15 plants, were used. Asterisk indicates significant differences with the wild-type plants (Student's *t*-test, $p < 0.05$). **(D)** Arsenic quantification in wild-type (Col-0) and *phif1-2* mutant plants. Plants were grown as in (C) and then exposed to 30 µM As(V) in liquid conditions for 24 h. For the quantification the whole plant was used in each case. Three independent biological replicas, each with 100 plants were used. Asterisk indicates significant differences with the wild-type (Col-0) plants (Student's *t*-test, $p < 0.05$). **(E)** As(V) tolerance phenotype of wild-type plants and *phif1-2* mutant. Plants were grown in horizontal plates containing 10 µM Pi alone (control) or in combination with 15 µM As(V), for 8 days. **(F)** Relative root growth quantification (ratio of primary root length of each individual in control or As(V) supplemented plates, relative to the average of the primary root length of the corresponding genotype in control conditions) in wild-type and *phif1-2* mutant plants from the experiment shown in (E). Roots from at least 15 plants were quantified in each case. Error bars indicate SD. Double asterisk indicates significant differences with the wild-type (Col-0) plants (Student's *t*-test, $p < 0.001$).

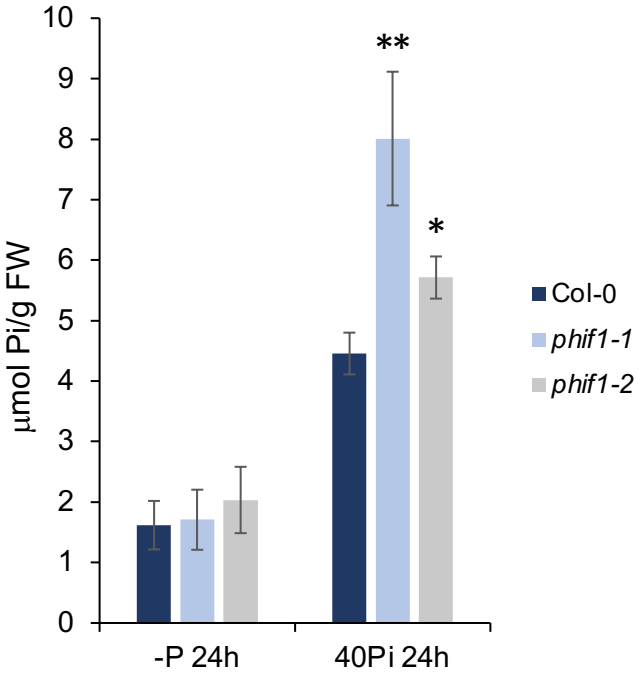

Supplemental Figure 12. Cellular free phosphate content in *phif1* T-DNA insertion mutants. Wild-type (Col-0), *phif1-1* and *phif1-2* plants were grown on solid Johnson medium supplemented with 1 mM Pi in horizontal position for 7 days, transferred to low Pi medium for 4 days, and subsequently transferred to Johnson plates containing 0 or 40 µM Pi for 24h. The method of Ames was used to determine the cellular phosphate content (Ames, 1966). The concentration of free phosphate per sample was normalized by the sample fresh weight (FW). Three independent biological replicas, each consisting of 15 plants, were used. Asterisk and double asterisk indicate significant differences with the wild-type (Student's *t*-test, $p < 0.05$ and $p < 0.01$), respectively.

Supplemental Table 1. ASK18 putative interactors described in the three *Arabidopsis* interactor databases (BAR PPI, BioGRID and IntAct) (Geisler-Lee et al., 2007; Dong et al., 2019). The seven common putative interactors among the three databases are annotated at the end of the table.

AGI	Gene Annotation	Database
At1g09650	F-box and associated interaction domains-containing protein	BAR PPI
At3g61590	**HWS Galactose oxidase/kelch repeat superfamily protein**	
At3g21130	F-box and associated interaction domains-containing protein	
At3g22940	F-box associated ubiquitination effector family protein	
At3g23880	F-box and associated interaction domains-containing protein	
At3g24580	F-box and associated interaction domains-containing protein	
At3g24760	Galactose oxidase/kelch repeat superfamily protein	
At3g54460	SNF2 domain-containing protein	
At3g57580	F-box and associated interaction domains-containing protein	
At3g58940	F-box/RNI-like superfamily protein	
At3g63060	EDL3 EID1-like 3	
At3g17540	F-box and associated interaction domains-containing protein	
At4g02570	ATCUL1 cullin 1	
At4g05460	AtSKIP19 RNI-like superfamily protein	
At4g08980	FBW2 F-BOX WITH WD-40 2	
At4g12560	CPR1 F-box and associated interaction domains-containing	
At4g19930	F-box and associated interaction domains-containing protein	
At4g19940	F-box and associated interaction domains-containing protein	
At4g39760	Galactose oxidase/kelch repeat superfamily protein	
At5g41490	F-box associated ubiquitination effector family protein	
At5g49000	**Galactose oxidase/kelch repeat superfamily protein**	
At3g18320	F-box and associated interaction domains-containing protein	
At3g17490	F-box and associated interaction domains-containing protein	
At1g11270	F-box and associated interaction domains-containing protein	
At1g76830	F-box and associated interaction domains-containing protein	
At1g18150	ATMPK8 Protein kinase superfamily protein	
At1g21410	SKP2A F-box/RNI-like superfamily protein	
At1g23390	KFB Kelch repeat-containing F-box family protein	
At1g31350	KUF1 KAR-UP F-box 1	
At1g47340	F-box and associated interaction domains-containing protein	
At1g53790	F-box and associated interaction domains-containing protein	

At1g60570	Galactose oxidase/kelch repeat superfamily protein	
At1g70590	F-box family protein	
At2g07140	F-box and associated interaction domains-containing protein	
At3g16580	F-box and associated interaction domains-containing protein	
At2g14710	F-box family protein	
At2g16220	F-box and associated interaction domains-containing protein	
At2g25490	EBF1 EIN3-binding F box protein 1	
At3g03360	F-box/RNI-like superfamily protein	
At3g06240	F-box family protein	
At3g08750	F-box and associated interaction domains-containing protein	
At3g10430	F-box and associated interaction domains-containing protein	
At3g13820	F-box and associated interaction domains-containing protein	
At3g13830	F-box and associated interaction domains-containing protein	
At5g49610	**F-box family protein**	
At3g63060	EDL3 EID1-like 3	BioGRID
At3g61590	**HWS Galactose oxidase/kelch repeat superfamily protein**	
At5g49610	**F-box family protein**	
At4g02570	ATCUL1 cullin 1	
At1g31350	KUF1 KAR-UP F-box 1	
At5g49000	**Galactose oxidase/kelch repeat superfamily protein**	
At4g12560	CPR1 F-box and associated interaction domains-containing	
At1g09650	F-box and associated interaction domains-containing protein	
At1g11270	F-box and associated interaction domains-containing protein	
At1g21410	SKP2A F-box/RNI-like superfamily protein	
At1g23390	KFB Kelch repeat-containing F-box family protein	
At1g47340	F-box and associated interaction domains-containing protein	
At1g53790	F-box and associated interaction domains-containing protein	
At1g60570	Galactose oxidase/kelch repeat superfamily protein	
At1g70590	F-box family protein	
At1g76830	F-box and associated interaction domains-containing protein	
At2g07140	F-box and associated interaction domains-containing protein	
At2g14710	F-box family protein	
At2g16220	F-box and associated interaction domains-containing protein	
At2g25490	EBF1 EIN3-binding F box protein 1	
At3g06240	F-box family protein	
At3g08750	F-box and associated interaction domains-containing protein	
At3g10430	F-box and associated interaction domains-containing protein	

At3g13820	F-box and associated interaction domains-containing protein	
At3g13830	F-box and associated interaction domains-containing protein	
At3g16580	F-box and associated interaction domains-containing protein	
At3g17490	F-box and associated interaction domains-containing protein	
At3g17540	F-box and associated interaction domains-containing protein	
At3g18320	F-box and associated interaction domains-containing protein	
At3g21130	F-box and associated interaction domains-containing protein	
At3g22940	F-box associated ubiquitination effector family protein	
At3g23880	F-box and associated interaction domains-containing protein	
At3g24580	F-box and associated interaction domains-containing protein	
At3g24760	Galactose oxidase/kelch repeat superfamily protein	
At3g54460	SNF2 domain-containing protein / helicase domain-containing	
At3g57580	F-box and associated interaction domains-containing protein	
At3g58940	F-box/RNI-like superfamily protein	
At4g05460	AtSKIP19 RNI-like superfamily protein	
At4g08980	FBW2 F-BOX WITH WD-40 2	
At4g19930	F-box and associated interaction domains-containing protein	
At4g19940	F-box and associated interaction domains-containing protein	
At4g39760	Galactose oxidase/kelch repeat superfamily protein	
At5g41490	F-box associated ubiquitination effector family protein	
At3g03360	F-box/RNI-like superfamily protein	
At3g63060	EDL3 EID1-like 3	IntAct
At5g49000	**Galactose oxidase/kelch repeat superfamily protein**	
At3g61590	**HWS Galactose oxidase/kelch repeat superfamily protein**	
At1g31350	KUF1 KAR-UP F-box 1	
At4g02570	ATCUL1 cullin 1	
At2g25490	EBF1 EIN3-binding F box protein 1	
At4g38940	Galactose oxidase/kelch repeat superfamily protein	
At5g49610	**F-box family protein**	
At3g54650	FBL17 RNI-like superfamily protein	
At3g61590	**HWS Galactose oxidase/kelch repeat superfamily protein**	Common
At3g63060	EDL3 EID1-like 3	
At4g02570	ATCUL1 cullin 1	
At5g49000	**Galactose oxidase/kelch repeat superfamily protein**	
At1g31350	KUF1 KAR-UP F-box 1	
At2g25490	EBF1_FBL6_EIN3-binding Fbox protein 1	
At5g49610	**F-box family protein**	

Supplemental Table 2. Primers used in this study

Name	Primer sequence 5´-3´	Usage
ASK18_for	CACCATGGCTTCTTCTTCCGAAGAG	pENTR-D-Topo vector construction
ASK18_rev	TTACTCATTAAAAGTCCAAGCA	
PHR1_for	CACCATGGAGGCTCGTCCAGTTCATAG	
PHR1_rev	TCAATTATCGATTTTGGGACGC	
AT5G49000_for	CACCATGTCGTCTCCAGAGAGGAAGA	
AT5G49000_rev	TCAAAGAGTAGCAGCAAGAGC	
AT5G49610_for	CACCATGGATAACCAAAAAGGTGCTC	
AT5G49610_rev	TTAATTACAGGGTACTATGGTGCTG	
AT3G63060_for	CACCATGCTTCTAGAGGGAAGATTC	
AT3G63060_rev	TTAGATCACACTTCCGTCCAC	
AT3G61590_for	CACCATGGAAGCAGAAACGTCTTGG	
AT3G61590_rev	CTAAGGAGCAATCTCGAGTCTTG	
AT2G25490_for	CACCATGTCTCAGATCTTTAGTTTTGC	
AT2G25490_rev	TCAGGAGAGGATGTCACATTT	
AT1G31350_for	CACCATGGAAAAAAAACTGAAACGGC	
AT1G31350_rev	TCAGCAAAAATTCGGTTGAC	
ask18-1_LP	CTACAATCGGATTCCTGATCG	T-DNA mutant genotyping
ask18-1_RP	ATGTAATCAGCAACCGTCTGG	
ask18-2_LP	ATGTAATCAGCAACCGTCTGG	
ask18-2_RP	GTTGATCATCATCCAAGACGG	
phif1-1_LP	TCTGCAAGTCGGAGTAGAAGC	
phif1-1_RP	CAAATGTGTGTGCCTCGTATG	
phif1-2_LP	AAGTTGTTGTTTCAACCGGTG	
phif1-2_RP	GAGCTCTCGAACCCTCGTTAC	
LBb1.3	ATTTTGCCGATTTCGGAAC	
GK_LB_o8474	ATAATAACGCTGCGGACATCTACATTTT	
PHT1;1_q_for	CCTCAACTCTCCAGAGAAGTTCTTA	Gene expression analysis
PHT1;1_q_rev	TTCGGCCATTTCCTAGAGC	
PHO1_q_for	TTTCCAACTCAGAAAAACCAG	
PHO1_q_rev	GTCATCCCCAGTTTCTGAGC	
WRKY6_q_for	GCAACAGCAACAACAGAACAA	
WRKY6_q_rev	ACACATCCTCGGCCTCAC	
PHR1_q_for	CTGCTGATTCGAAGGAGGTT	
PHR1_q_rev	GCTTTGGCTGTGGAGATTCTA	
ASK18_q_for	TCAACATCGAGAACGATTTCAC	
ASK18_q_rev	AAGCATTCTCCTTGCGAATC	
At4_q_for	TGGCCCCAAACACAAGAG	
At4_q_rev	CGAACATTCACAATCATAATCTCC	
SQD1_q_for	GGGACTCTCAACGTTCTCTTTG	
SQD1_q_rev	CCCATCGTCCCAAGTTTTAC	
RNS1_q_for	TTGTTATCCAAATTCAGGCAAA	
RNS1_q_rev	AGTTAGGCCAAAGACCATGAAT	
EF1a_q_for	CCCAGGCTGATTGTGCTGT	
EF1a_q_rev	TTCGGCCATTTCCTAGAGC	
ACT8_q_for	GACTCAGATCATGTTTGAGACCTTT	
ACT8_q_rev	CCAGAGTCCAACACAATACCG	
AT5G49000_for	ATGTCGTCTCCAGAGAGGAAGA	
AT5G49000_rev	TCAAAGAGTAGCAGCAAGAGC	